

3-10-2010

Particulate Characterization and Control Evaluation for Carbon Fiber Composite Aircraft Crash Recovery Operations

Matthew R. Ferreri

Follow this and additional works at: <https://scholar.afit.edu/etd>



Part of the [Toxicology Commons](#)

Recommended Citation

Ferreri, Matthew R., "Particulate Characterization and Control Evaluation for Carbon Fiber Composite Aircraft Crash Recovery Operations" (2010). *Theses and Dissertations*. 2134.
<https://scholar.afit.edu/etd/2134>

This Thesis is brought to you for free and open access by the Student Graduate Works at AFIT Scholar. It has been accepted for inclusion in Theses and Dissertations by an authorized administrator of AFIT Scholar. For more information, please contact richard.mansfield@afit.edu.



**PARTICULATE CHARACTERIZATION AND CONTROL EVALUATION FOR
CARBON FIBER COMPOSITE AIRCRAFT CRASH RECOVERY
OPERATIONS**

THESIS

Matthew R. Ferreri, Captain, USAF, BSC, CIH

AFIT/GIH/ENV/10-M01

**DEPARTMENT OF THE AIR FORCE
AIR UNIVERSITY**

AIR FORCE INSTITUTE OF TECHNOLOGY

Wright-Patterson Air Force Base, Ohio

APPROVED FOR PUBLIC RELEASE; DISTRIBUTION UNLIMITED

The views expressed in this thesis are those of the author and do not reflect the official policy or position of the United States Air Force, the Department of Defense, or the United States Government.

AFIT/GIH/ENV/10-M01

PARTICULATE CHARACTERIZATION AND CONTROL EVALUATION FOR
CARBON FIBER COMPOSITE AIRCRAFT CRASH RECOVERY OPERATIONS

THESIS

Presented to the Faculty

Department of Systems and Engineering Management

Graduate School of Engineering and Management

Air Force Institute of Technology

Air University

Air Education and Training Command

In Partial Fulfillment of the Requirements for the

Degree of Master of Science in Industrial Hygiene

Matthew R. Ferreri, BS

Captain, USAF, BSC, CIH

March 2010

APPROVED FOR PUBLIC RELEASE; DISTRIBUTION UNLIMITED

PARTICULATE CHARACTERIZATION AND CONTROL EVALUATION FOR
CARBON FIBER COMPOSITE AIRCRAFT CRASH RECOVERY OPERATIONS

Matthew R. Ferreri, BS
Captain, USAF, BSC, CIH

Approved:

//SIGNED//

1 Mar 2010

Maj Jeremy M. Slagley (Chairman)

Date

//SIGNED//

18 Feb 2010

Lt Col David A. Smith (Member)

Date

//SIGNED//

18 Feb 2010

Daniel L. Felker, PhD (Member)

Date

Abstract

Within the United States Air Force (USAF) Advanced Composite Material (ACM) is gaining an increasing use in military aircraft. With the number of aircraft that have increasingly large amounts of ACM materials, the probability of an incident with one of these aircraft also increases. When such an incident occurs the aircraft needs to be disassembled, removed, and later inspected as part of the accident investigation process. This disassembly process is termed “Crash Recovery Operations.” Carbon fibers have been shown to be hazardous to human health and a pilot study raised the suspicion that nanosized aerosol may be generated during the cutting of carbon fiber panels. Due to this, a bench top study was conducted to evaluate the effectiveness of several fiber controls. Additionally, an evaluation of a number of direct reading instruments and traditional gravimetric sampling techniques were evaluated to determine a sampling protocol for evaluation composite fibers. A statistically significant (F-value = < 0.0001) shift towards larger diameters in the idealized particle size distribution was shown for both wetted water and water controls when compared to a baseline of no control when cutting burnt ACM. Recommendations for future evaluation and control of composite fiber processes were made.

Acknowledgments

I would like to thank my beautiful wife for her love and patience during this stressful 18-month endeavor. During this time, I have often been less than pleasant but you have always been at my side and never wavered in your love and support. I would have not been able to complete this document without your tireless editing efforts.

I would also like to thank Major Jeremy Slagley. Your guidance and encouragement, while painful at times, helped to produce what I believe is a quality product. Please, no more midnight drives to San Antonio.

My gratitude also extends to my thesis committee. Dr. Felker, I would not have been able to put together my experimental setup without your assistance. To Lt Col Smith, thank you for your instruction, encouragement, and review of this document. I would like to add it took longer than 20 minutes to meet my Major's board.

I also would like to thank the 445 Airlift Wing Fuels Element, 88 Airbase Wing Fire and Emergency Services Flight, AFRL Materials Directorate, Air Force Advanced Composite Office, Wright-Patterson BEE Flight, and USAFSAM for their help procuring the materials and supplies needed to perform this study.

Matthew Ferreri

Table of Contents

	Page
Abstract.....	iv
Acknowledgments.....	v
List of Figures.....	viii
List of Tables.....	x
List of Abbreviations.....	xi
I. Introduction.....	1
Problem Statement.....	2
Research Objectives.....	3
Methodology.....	4
II. Literature Review.....	5
Carbon Fiber Toxicity.....	5
Nanoparticle Toxicity.....	9
CNT Toxicity.....	10
What to Sample.....	12
HAMMER Studies.....	14
Mass.....	16
NIOSH NEAT Method.....	18
OPC.....	19
CPC.....	20
Measurements.....	21
Surface Area.....	22
Problem Statement.....	23
III. Method.....	25
Ticket Heat Treatment.....	25
Cut experiment.....	27
Instrument Setup.....	33
Surface Area Meter.....	33
CPC.....	33
OPC.....	34
Gravimetric.....	34
SEM Sample prep.....	35

	Page
Analysis	36
IV. Results.....	39
V. Discussion/Conclusions	52
Introduction.....	52
Intact Tickets	52
Burnt Tickets	54
Overall Impressions	56
Idealized Particle Size Distribution	58
Respirable Fraction	60
Water.....	64
Wetted Water	64
Wax.....	64
AFFF.....	65
SEM	65
Pretreatment Effectiveness.....	66
Potential Controls.....	67
Sampling Methodology Improvements	68
Future Studies	72
Recommendations for BE Flights.....	77
Conclusions.....	78
Appendix A.....	81
Appendix B	84
Detailed Procedures	84
Cut Procedure.....	84
SEM Sample prep	85
Appendix C	87
Bibliography	90

List of Figures

	Page
Figure 1 ACM ticket burn orientation	25
Figure 2 Burning ACM ticket	26
Figure 3 ACM ticket after burn with obvious signs of delamination	27
Figure 4 Experiment setup	28
Figure 5 Dremel tool setup during cut experiments.....	29
Figure 6 Sampling setup	30
Figure 7 Burnt ticket post cut with obvious flaking off of material due to delamination.	32
Figure 8 Typical wide view of carbon foil with sample (burnt ACM with a wetted water control)	45
Figure 9 Partially decomposed carbon fiber from an intact ACM sample with no control	46
Figure 10 Overlapping partially decomposed carbon fibers from an intact ACM sample with a wetted water control.....	47
Figure 11 Carbon fiber with filament attached from a burnt ACM sample with no control	48
Figure 12 Close-up of filament from a burnt ACM sample with no control	49
Figure 13 Close-up view of fiber with particle attached.....	50
Figure 14 Carbon particle with sub micron filament protruding (burnt ACM with a wetted water control)	51
Figure 15 JMP 8.0 Tukey's HSD post test grouping for surface area monitor	53
Figure 16 JMP 8.0 ANOVA of CPC count/cc metric for burnt tickets	55
Figure 17 Burnt OPC+CPC CMD using strategy 3 ANOVA table.....	57
Figure 18 Intact OPC+CPC CMD using strategy 3 ANOVA table.....	57
Figure 19 Burnt respirable fraction ANOVA table.....	57
Figure 20 Intact respirable fraction ANOVA table.....	57
Figure 21 Plot of idealized particle size distributions for burnt tickets based on CMD and CMD GSD (strategy 3) for different control options.....	58
Figure 22 Idealized particle size distribution ANOVA table.....	60
Figure 23 Tukey's HSD grouping of idealized particle size distributions	60
Figure 24 Respirable deposition percentage along with settling size a 5 time hacks	62
Figure 25 Diagram of interaction area of blade and control for intact tickets (blue) as compared to interaction of blade and burnt tickets (red)	67
Figure 26 Plot of idealized particle size distributions for intact tickets based on CMD and CMD GSD (strategy 1) for different control options.....	87
Figure 27 Plot of idealized particle size distributions for burnt tickets based on CMD and CMD GSD (strategy 1) for different control options.....	87
Figure 28 Plot of idealized particle size distributions for intact tickets based on CMD and CMD GSD (strategy 2) for different control options.....	88
Figure 29 Plot of idealized particle size distributions for burnt tickets based on CMD and CMD GSD (strategy 2) for different control options.....	88

Figure 30 Plot of idealized particle size distributions for intact tickets based on CMD and CMD GSD (strategy 3) for different control options..... 89

List of Tables

	Page
Table 1 Fiber/Particulate task exposure concentrations during the recovery phase	15
Table 2 Average respirable and total mass concentration results with standard deviation (mg/m ³)	39
Table 3 Respirable fraction averages with standard deviation	40
Table 4 Average CPC results with standard deviation (count/cc)	41
Table 5 Average surface area meter results with standard deviation (μm ² /cc)	42
Table 6 Average CMD and MMD values with standard deviation for OPC particle size distribution data (μm)	43
Table 7 CMD and MMD using both OPC and CPC with strategy one (μm)	43
Table 8 CMD and MMD using both OPC and CPC with strategy two (μm)	44
Table 9 CMD and MMD using both OPC and CPC with strategy three (μm)	45
Table 10 Settling distances at 2, 5, 10, 15, and 20 minute marks for multiple particle diameters	61
Table 11 Settling threshold at 5 time hacks	62
Table 12 Percent of original mass aloft at 5 time hacks	63
Table 13 Areas of sampling strategy for composite fiber this study satisfies	72
Table 14 Importance of different areas of potential sampling prior to this study	73
Table 15 Priority of future sampling of ACM within the Air Force	74
Table 16 CPC, Surface Area, Respirable Mass Concentration, Total Mass Concentration, and Respirable Fraction data used for statistics	81
Table 17 OPC CMD, OPC MMD, OPC+CPC CMD (Strategy 1), and OPC+CPC MMD (Strategy 1) data used for statistics	82
Table 18 OPC+CPC CMD (Strategy 2), OPC+CPC MMD (Strategy 2), OPC+CPC CMD (Strategy 3), OPC+CPC MMD (Strategy 3) data used for statistics	83

List of Abbreviations

ACGIH	American Conference of Governmental Industrial Hygienists
ACM	Advance Composite Material
AFB	Air Force Base
AFFF	Aqueous Film Forming Foam
ANOVA	Analysis of Variance
BMI	Bismaleimide
CMD	Count Media Diameter
CNT	Carbon Nanotube
CPC	Condensation Particle Counter
DRI	Direct Reading Instrument
EAD	Electrical Aerosol Detector
GSD	Geometric Standard Deviation
HAMMER	Hazardous Aerospace Material Mishap Emergency Response
HEPA	High Efficiency Particulate Air
LEV	Local Exhaust Ventilation
MCE	Mixed Cellulose Ester
MMD	Mass Median Diameter
MWCNT	Multi Walled Carbon Nanotubes
MPPS	Most Penetrating Particle Size
NEAT	Nanoparticle Emission Assessment Technique
NIOSH	National Institute for Occupation Health and Safety

OPC	Optical Particle Counter
PPE	Personal Protective Equipment
PVC	Polyvinyl Chloride
SWCNT	Single Walled Carbon Nanotubes
TEM	Transmission Electron Microscopy
TLV	Threshold Limit Value
TO	Technical Order
SEM	Scanning Electron Microscopy

PARTICULATE CHARACTERIZATION AND CONTROL EVALUATION FOR CARBON FIBER COMPOSITE AIRCRAFT CRASH RECOVERY OPERATIONS

I. Introduction

Within the United States Air Force, Advanced Composite Material (ACM) is gaining an increasing use within military aircraft. The F-16 and F-15 fighters were developed in the 1970s are comprised of 13 and 1.6 percent ACM materials respectively. Recent additions to the inventory such as the B-2 Spirit and F-22 Raptor are composed of 37 and 38 percent ACM materials respectively. The forthcoming F-35 Lightning II is also comprised of a large amount of ACM panels with 29 percent of the aircraft being composite. (Air Force Advanced Composites Office) In addition to ACM skin panels used on older aircraft, there are several structural members in the F-35 that are comprised of ACM. With the number of aircraft that have increasingly large amounts of ACM materials, the probability of an incident with one of these aircraft also increases.

Such an incident occurred on February 23, 2008, when a B-2 crashed on takeoff at Andersen Air Force Base (AFB), Guam. Once the fire had been extinguished there was a need to remove the airframe from the runway so that it could be returned to service. Within the Air Force this is termed “Crash Recovery Operations.”

Crash recovery is a tasking that occurs in-garrison as well as at deployed locations. When aircraft crash in-garrison there is a deliberate process by which the incident is managed. Once immediate safety issues are addressed, a safety board is convened to investigate the cause of the crash. Once this has occurred, members of the board will enter the crash site to retrieve evidence and document the scene. This is done

so a cause can be determined and actions can be taken to prevent future crashes. Also, during the safety board investigation the aircraft is removed from the crash site.

To remove the aircraft, crash recovery personnel cut the airframe into sections that will fit onto a standard flat-bed trailer (~15 m). The workers commonly use gas-powered concrete saws. The wings and the tail section of the airframe are always removed. Depending on the size, the main fuselage may need to be cut into sections that can also fit onto a flat-bed trailer.

At an active deployed airfield this process happens much faster than in-garrison. This is due to the need to put the airfield back into operation so that aircraft can be launched and recovered in support of directives given by the Combatant Commander. In order to return the runway to operational status the aircraft will either be moved off of the runway to be disassembled or will be quickly disassembled in place.

In the case of the B-2 incident in Guam, maintenance personnel disassembled the aircraft so the Andersen AFB runway could return to operational status as quickly as possible. The workers were closely monitored and wore the appropriate Personal Protective Equipment (PPE) during the entire operation. However, size distribution, surface area, and mass concentration measurements were not taken during the crash recovery operation to determine the precise exposure during the aircraft disassembly. (Cayce, O'Sullivan, & Lujan, 2008)

Problem Statement

Current Air Force guidelines regarding the hazards of composite fibers were written in 2001. This document written by the Air Force Institute for Environment,

Safety, and Occupational Health Risk Analysis (AFIERA) published guidance for Bioenvironmental Engineers (BE) so they could make recommendations to the commander during a composite fiber incident. The report explained the risk presented by ACM panels, how to evaluate those risks, and the protective measures to be taken to reduce exposures to workers in and around aircraft crashes. (AFIERA, 2001) This report provided PPE and sampling guidance for BEs in the field but did not utilize Direct Reading Instruments (DRIs) which have gained acceptance since its publication in 2001. DRIs such as the Optical Particle Counter (OPC), Condensation Particle Counter (CPC), and surface area monitor have become valued assets in the assessment of aerosol environments. These DRIs can be used by the BEs to better evaluate the hazards present during crash response and crash recovery operations. In turn, a better control decision can be made along with a better exposure record for workers that may have been exposed.

The BE guidance document was drafted using the information gathered during previous crashes as well as the Hazardous Aerospace Material Mishap Emergency Response (HAMMER) study conducted in 2000 and published in 2001 (AFIERA, 2001). This study also did not utilize modern DRIs for its evaluation of the ACM hazard.

Research Objectives

The objectives of this thesis are:

1. Evaluation of four different potential controls' effectiveness at reducing exposure to composite fiber particulate aerosolized during the cutting of ACM panels.

2. Determination of better sampling procedures for evaluating exposure to composite processes.

Methodology

To satisfy these objectives a series of small bench top experiments were performed using a number of gravimetric measurements and DRI instruments to evaluate cutting of burnt and intact ACM panels. These experiments included the cutting of both burnt and intact ACM tickets using different controls and comparing results obtained with a baseline of no control application.

II. Literature Review

With the large number of Air Force aircraft which include ACM panels, the health hazard posed by these materials is of concern. ACM panels are composed of laminated plies of woven fibers bound within a polymer resin. (Kimmel & Courson, 2002) Within the Air Force, carbon and boron are the most common fibers used where epoxy and bismaleimide (BMI) are the most common resins. Carbon fibers are typically formed by heat treating of cellulose or polyacrylonitrile. (Proctor & Sherwood, 1982) Carbon fibers used within the ACM typically have a diameter on the order of 7-10 μm . While this size is not respirable, some studies have shown that during a fire the fibers are reduced in size due to oxidation and fibrillation. (Sussholtz, 1980)

Carbon Fiber Toxicity

In 2009, Adrian Mouritz conducted an extensive literature review of the toxicity of composite fibers. In the review Mouritz noted the following information. Medical research has shown that the toxicity of mineral fibers such as asbestos and quarts are highly dependent on the concentration and size of their fibers. As a rule of thumb, the toxicity of the fibers increases with fiber concentration when the fibers fall within a specific size range. Due to these facts, studies were conducted to determine the nature of the fiber and particulates released when carbon fiber composites are burned. These studies were primarily conducted using graphite-epoxy composites and not graphite-BMI composites. Mouritz noted that more work is needed to determine the fiber and particulate release in different composite fiber formulations. (Mouritz, 2009)

The toxicity studies on composite fibers were conducted using virgin fibers that have a typical size range of 7-10 μm . The toxicity of burnt fibers can be very different than the toxicity of virgin fibers though they will likely shed some light on the toxicity of the burnt fibers. This difference in toxicity is due to the fact that the fibers will be contaminated with combustion byproducts and residual resin used to bind the fibers together. Additionally, the fibers released during fires range from single fibers to fragments which are composed of hundreds of fibers. (Mouritz, 2009)

Gandhi *et al.* also conducted a literature review of the health hazards of burning aircraft composites. Gandhi *et al.* stated that carbon fibers pose both a dermal contact hazard and an inhalation hazard. The composite fibers pose the highest inhalation risk when they are 2-3 μm in diameter as they are able to pass through the respiratory tract and enter the pulmonary region of the lungs. This ability to enter the pulmonary region becomes zero as the fiber's diameter approaches 7-10 μm . Fibers with lengths outside the typical respirable range are able to enter the pulmonary region due to the fact that when composite fibers enter the airstream of the respiratory tract the fibers tend to align lengthwise with the airstream.(Gandhi, Lyon, & Speitel, 1999)

The studies reviewed by Gandhi *et al.* showed no long term or latent effects from carbon fiber exposure. These studies looked for asbestos and quartz like effects in the lungs due to carbon fibers. There were no studies that found fibrosis effects or changes in pulmonary function response. Gandhi *et al.* did note that some studies showed acute effects from carbon fibers. Fibers that penetrated to the pulmonary region of the lungs caused lesions and inflammation though far less than the control mice that were exposed to quartz. Additionally, dose dependent inflammatory response was noted in one study

but this inflammatory response reversed within 10 days of exposure. (Gandhi, Lyon, & Speitel, 1999)

Gandhi *et al.* noted that the current studies on carbon fiber toxicity have focused on long-term exposures that are typically found in occupational environments not single high dose exposures to carbon fibers. Also, these animal studies used virgin fibers rather than fibers produced from the burning of composites. The authors concluded that even with the lack of scientific evidence linking carbon fiber to asbestos like effects that it would be prudent for personnel involved in aircraft crash recovery and response to take precautionary measures. (Gandhi, Lyon, & Speitel, 1999)

Zhang *et al.* also conducted a study of the toxicity of carbon fibers and carbon fiber composite dust administered by intratracheal injection. The authors performed bronchoalveolar lavage to evaluate the response within the rats that were dosed. Zhang *et al.* noted that “Some fibres were apparently phagocytosed by 2 or more macrophages, with the longer fibres sometimes giving the appearance of a string of beads.” The carbon fiber and carbon fiber dust were not found in mice one month post exposure. Zhang *et al.* concluded the fibers and fiber dusts have been phagocytosed by macrophages. These macrophages showed no adverse effects due to the breakdown of the fibers and dusts. This is in contrast to the response of the control mice that were dosed with quartz and asbestos where the macrophages did show obvious signs of adverse effects including morphological changes and cellular debris due to cell death. (Zhang, et al., 2001)

In 1980, NASA conducted several studies on the burning of composite fiber materials. Their study showed that carbon fibers will decrease in size when they are burned. This reduction in size is due to two processes. One is the oxidation of the fibers

in the intense heat of the fire. The second is a phenomenon called fibrillation where the fibers actually break apart in the fire. A burn study was conducted at Dugway Proving Ground to study this fibrillation phenomenon. The study showed that of the released fibers 60% were what the author termed micron fibers where the fiber diameter was less than 3.0 μm . Of the micron fibers collected 21% had diameters ranging from 0.4–1.0 μm . The average diameter of the micron fibers collected was 1.5 μm . No count median diameter or mass media diameter information was presented. (Sussholtz, 1980)

A nanoparticle is defined as a particle having at least one dimension less than 100 nm. (NIOSH, 2009) The NASA study showed that a significant proportion of the fibers released from burning composites nearly fall within the nanoparticle definition. (Sussholtz, 1980) A US Air Force study showed that between 19.4% and 50.1% of the particles released from a composite fiber smoke plume are in 0-1 μm size range which overlaps the definition of a nanoparticle. (Courson, et al., 1996) These studies along with a pilot study conducted previously indicated the aerosol generated during cutting intact and burnt ACM panels may fall within the definition of a nanomaterial. (Ferreri, Slagley, & Felker, 2009) With this in mind the toxicology associated with nanoparticles is relevant to this work.

The evaluation of nanoparticle toxicity is fraught with uncertainty. Many size dependent characteristics that make nanoparticles so interesting to the engineering and medical professionals may change their toxicological characteristics as well. As stated by NIOSH, "...characteristics of nanoparticles may be different from those of larger particles with the same chemical composition." (NIOSH, 2009)

Nanoparticle Toxicity

Inhalation exposure is the most common route of exposure for chemicals and airborne particles including nanoparticles. Once the nanoparticle is inhaled, its shape and size will determine where in the respiratory tract it will deposit. If the nanoparticle has agglomerated, the shape and size of the agglomerate, not the constituent nanoparticle, will drive the deposition site within the respiratory tract. (NIOSH, 2009) Nanoparticles, due to their small size, are able to deposit in the alveolar region of the lungs. (ICRP, 1994)

Once deposited within the body, the nanoparticle will either be transported to a different area within the body to cause a reaction or will cause a reaction where it deposited. Oberdörster *et al.* showed that elemental ^{13}C particles that deposited in the nasal region of the respiratory tract were transported to the brain via the olfactory nerve. (Oberdörster, et al., 2004) Elder *et al.* showed similar transport of manganese oxide nanoparticles to the brain via the olfactory nerve. (Elder, et al., 2006)

Due to increased surface reactivity per unit mass it is anticipated that nanoparticles will exhibit greater biologic activity than particles of large size. In the respiratory tract, laboratory-generated model nanoparticles or ambient nanoparticles have been shown to contribute to adverse health effects. Studies have shown significant inflammation as well as oxidative stress within the respiratory tract. This oxidative stress has been linked to changes in gene expression and cell signaling pathways. (Oberdörster, Oberdörster, & Oberdörster, 2005)

Beyond the inhalation route of exposure, other routes of exposure are also of concern for nanoparticles. Tinkle *et al.* showed that particles less than 1 μm in diameter

can pass through the stratum corneum when it is mechanically flexed. (Tinkle, et al., 2003) This ability to pass through the stratum corneum provides for a dermal route of exposure for nanoparticles. Additionally, nanoparticles that deposit within the upper respiratory tract move via the mucociliary escalator to be swallowed and present an ingestion route of exposure.

CNT Toxicity

Carbon Nanotubes (CNT) are a morphology of nanoparticles in which the thin sheet of carbon molecules is rolled to make a cylinder of pure carbon with a diameter on the order of 1.5 nm for single walled carbon nanotubes. (Maynard, 2006) This structure may be relevant to carbon fiber toxicity as the carbon fibers tend to reduce in diameter to sizes that nearly fall within the definition of a nanoparticle. (Sussholtz, 1980) Additionally, research is underway on infusing CNTs into carbon fiber composites.

Shvedova *et al.* have shown that exposure to single-walled carbon nanotubes (SWCNT) can produce epitheloid granulomas (Shvedova, et al., 2005), which can impair the gas exchange within the lungs. These results concur with the results of studies published by Lam *et al.* (Lam C. W., James, McCluskey, & Hunter, 2004) Locations of granulomas were associated with the deposition of the agglomerated SWCNT. In addition to granulomas, Shvedova *et al.* linked SWNCT exposure to fibrosis in the lungs as well as decreased pulmonary function. The fibrosis was found to be dose dependant and did not mimic the classic causes that have been put forth for fibrogenetic particles, as the fibrosis was not caused, "...by chronic inflammation and chronic activation of alveolar macrophage." Shvedova *et al.* also stated that the interstitial fibrotic response generated

by the SWCNTs was not well predicted on a mass basis by ultrafine carbon black or crystalline silica, a reference nanoparticle and a classic fibrogenic particle. The particular cause of the fibrotic response was not stated by Shvedova *et al.* (Shvedova, et al., 2005)

Lam *et al.* stated that CNTs have been demonstrated to be intrinsically toxic and that exposure to respirable SWCNTs poses a risk of causing lung lesions. (Lam C. W., James, McCluskey, Arepalli, & Hunter, 2006) Lam *et al.* in a previous study compared the toxic concentrations of SWCNTs, as determined within their study, to the PEL for synthetic graphite and showed that a worker exposed at the graphite PEL would "...likely develop serious lung lesions." They also concluded that on an equal-weight basis if SWCNTs reach the lungs they are more toxic than carbon black and quartz, which are recognized as serious chronic inhalation hazards. (Lam C. W., James, McCluskey, & Hunter, 2004) In addition to being more toxic than the carbon black and quartz, Nygaard *et al.* showed that SWCNTs increased allergic response more than spherical ultrafine carbon black particles. Carbon black was used in the comparison because the difference between carbon black particles and SWCNT particles is chemical structure as they are both comprised purely of carbon atoms. (Nygaard, Hansen, Samuelsen, Alberg, Marioara, & Løvik, 2009)

CNTs have also been compared structurally to asbestos fibers with a needle-like shape and high aspect ratio for both asbestos and CNTs driving the comparison. Due to these structural similarities it has been theorized that CNTs may behave like asbestos fibers when interacting with the mesothelium. Poland *et al.* performed a test of this theory comparing the pathogenicity of Multi Walled Carbon Nanotubes (MWCNTs) from several manufacturers to long-fiber amosite. They found that similarly to long-fiber

amosite, MWCNTs longer than 20 μm caused granulomas and inflammation. MWCNTs with lengths less than 20 μm did not produce a significant response. This study used the mesothelial lining of mice as a surrogate for a human chest cavity mesothelial lining. Additionally, the study introduced the fibers directly to the mesothelial lining and did not study if CNTs would be able to reach the mesothelial lining after an inhalation exposure. (Poland, et al., 2008)

What to Sample

With the knowledge that nanoparticles, CNTs, and carbon fibers are toxic and present a respirable hazard, an Industrial Hygienist needs to determine what the best measure of dose and exposure is. Classically, this has been accomplished with mass concentration as seen in American Conference of Governmental Industrial Hygienists Threshold Limit Values (ACGIH TLV). Carbon fibers and CNTs are comprised purely of carbon and are chemically identical to graphite but the graphite TLV specifically excludes graphite fibers. (ACGIH, 2009)

Nygaard *et al.* found that particle surface area, number, and diameter are better predictors of response within mice lungs. They found that particle number and diameter were good predictors but the surface area was the stronger predictor of response. They also found that particle mass was not able to predict response within the lungs of the mice. (Nygaard, Samuelsen, Aase, & Løvik, 2004)

Maynard and Kuempel have suggested that nanostructure and surface area may be the most important dose metric. They found that the toxicity of the nanomaterials may be more closely tied with their nanostructure rather than the diameter of the particles.

Maynard and Kuempel use the example of an agglomerated mass of SWCNTs perhaps micrometers in diameter while itself being too large to meet the definition of a nanoparticle, it will exhibit the structure of a CNT where it is able to interact with the body. In other words, the clump could be larger than the 100 μm definition of a nanoparticle. The individual CNTs will protrude from the clump and will interact with the cells with which they come into contact as a nanoparticle. Therefore, the relevant properties are those of a CNT not the properties of the micrometer sized clump of which they are part. Maynard and Kuempel showed in their work that the most predictive measure of lung tumors in rats exposed to nanoparticles was surface area not mass. (Maynard & Kuempel, 2005)

Due to these different theories there is still no agreement on the best metric for nanoparticle dose. NIOSH has stated that while toxicology research is under way, there is still little agreement on the best measurement technique for nanoparticles. NIOSH goes on to state that mass seems to be "...less important than particles size and shape, surface area, and surface chemistry (or activity) for some nanostructured materials." (NIOSH, 2009) Oberdörster *et al.* also stated that a clear dose metric had not been found and have recommended that mass, surface area, and particle number be measured when gathering data on nanoparticles. When all three of these parameters are measured a determination of the best dose metric can be determined by which parameter is the most associated with the response. (Oberdörster, et al., 2005)

Due to the lack of a dose metric and the early state of toxicology studies, NIOSH has recommended that nanoparticle exposure should be minimized when possible. (NIOSH, 2009) Mazzuckelli *et al.* recommend that even with the lack of an accepted

personal exposure limit engineering controls should be used to reduce exposures to nanoparticles. (Mazzuckelli, et al., 2007) Current Air Force guidance states that acrylic floor wax mixed 2:1 with water should be applied to the surface of ACM panels after an aircraft crash in an attempt to suppress the suspension of ACM particles. The purpose of the wax is to act as a fixant and prevent the suspension of fibers and particles. (US Air Force, 2008) Discussions with the Advanced Composite Office at Hill AFB, Utah, indicated that the fixant effectiveness of this acrylic wax solution has not been fully evaluated. (Frank, 2009) Other potential controls at an aircraft crash site include a water mist, which is commonly used for dust suppression at construction sites and is readily available at aircraft crash sites. Wetted water could also be used as it is commonly used to reduce exposures to asbestos fibers. Another potential control is aqueous film-forming foam, commonly termed AFFF, which is also readily available at aircraft crash sites.

HAMMER Studies

In 2001, in response to a Safety Investigation Board finding, a study was performed to evaluate the hazards produced during ACM panel burning in aircraft mishaps. This study evaluated the burn products released during combustion of ACM panels. This study measured chemical releases as well as particulate and fiber releases during the combustion of an ACM panel. (AFIERA, 2001)

This study found that the only significant fiber release occurred during the post recovery operations while crash recovery operations were taking place. Respirable dust and total dust readings were also taken during the Initial Response/Safety Investigation Board (IR/SIB) and recovery phase operations. Table 1 shows the results of fiber,

respirable mass, and total mass samples during the recovery phase of the crash recovery from the HAMMER study. (AFIERA, 2001)

Table 1 Fiber/Particulate task exposure concentrations during the recovery phase

Team	Analyte	Recovery
		20-Sept-00
Team1	Fiber	0.41 f/cc
	Respirable dust	0.001 mg/m ³
	Total dust	0.0035 mg/m ³
Team2	Fiber	0.26 f/cc
	Respirable dust	0.0004 mg/m ³
	Total dust	0.004 mg/m ³
Team 3	Fiber	0.38 f/cc
	Respirable dust	0.0005 mg/m ³
	Total dust	0.003 mg/m ³

The HAMMER studies looked at a 20 pound sample of ACM cut from the wing box of a Navy A-6 (Costantino, 2010) donor aircraft and did not use any controls during the evaluation of the fiber and particulate release. The study states that “...exposures could be greater during real-world recovery operations. This is especially the case for aircraft such as the F-22, C-17, or B-2.” (AFIERA, 2001)

Further assessments of how to respond to composite aircraft crashes were also performed as part of the HAMMER studies. It was found that a fire during an aircraft crash will burn off some portion of the resin that binds the carbon fibers together. This will allow the material to more easily become airborne and present a potential hazard. Additionally, the aircraft will not burn evenly, “...there will be a gradation of the fire damage for the various aircraft parts.” Though not supported in the data presented, the report asserts that composite material not burnt during the crash will present less of a risk than that of the burnt sections. (AFIERA, 2001)

Mass

Traditionally, mass concentration has been the metric used to characterize dose to hazardous particles. NIOSH has stated that mass may not be the best metric to characterize the exposure to nanoparticles. Properties such as surface area and particle size may be better metrics of the nanoparticle dose. (NIOSH, 2009) Using standards such as carbon black or synthetic graphite as a limit for CNTs is not recommended as CNTs are not toxicologically equivalent to these compounds. (Lam C. W., James, McCluskey, Arepalli, & Hunter, 2006) Nonetheless, mass concentration is the only standard that is available for comparison when utilizing nanomaterials. Oberdörster *et al.* have recommended that mass concentration should be just one of the metrics used for the evaluation of nanoparticle dose. (Oberdörster, et al., 2005)

Within mass concentration, respirable mass concentration is often used when evaluating respirable hazards. Many hazardous chemicals have different effects based on where they have deposited in the respiratory tract. This is due to the fact that particle size affects where particles deposit within the respiratory tract. (ACGIH, 2009) Due to these facts, total mass samples can be filtered so that only the respirable mass fraction is collected.

To accomplish this, a two-stage respirable dust sampler is used. The first stage only allows the respirable fraction of particles to pass through and the second stage collects these particles for later analysis. A cyclone is used to reduce the sample to only the respirable mass. The cyclone works well to filter out the coarse particles within the sample, thereby leaving the respirable particles to pass through and be captured on the filter. As the air enters the cyclone a vortex is created. The air flows down the cyclone

and then reverses, a second vortex occurs as the air flows up the center portion of the cyclone. The larger particles are not able to follow the flow lines of the air in this double vortex due to their inertia and fall out. This cut point is set by the air flow rate through the cyclone. (Cohen & Charles S. McCammon, 2001)

The major limitation of the cyclone is that the cut curve of the cyclone does not precisely match up with the ACGIH respirable curve (Trakumas & Hall, 2003). Another limitation is that the cyclone needs a constant flow rate. Modern diaphragm pumps that compensate for filter loading tend to have a pulsating flow which degrades the cut point of the cyclone. Additionally, cyclones are sensitive to flow rate variation. That is, the cut point for the cyclone is very closely tied to the flow rate of the pump to which it is attached. If the pump is not precisely calibrated to the specified flow the cut point will be altered. (Cohen & Charles S. McCammon, 2001)

Once the sample has been reduced down to the respirable mass the particles are collected on a filter. In the case of mass sampling where mass and microscopic analysis is required matched weight filters can be used. In this case a Mixed Cellulose Ester (MCE) filter is used. The MCE filter is a membrane filter where a thin membrane with a specific pore size captures the sample on the surface of the filter. The filters are able to efficiently capture particles smaller than their pore size which has been linked to the diffusion and inertia of the particles in question. The fact that the sample is collected on the surface allows for microscopic analysis to occur as the mass collected is not embedded deep within the filter but rather on the surface. (Cohen & Charles S. McCammon, 2001)

The capture of the sample on the surface of the filter is also a limitation. Due to the fact that the sample is collected on the surface, the filter can be overloaded to the point where the sample cannot be visually analyzed. Additionally, particles that are collected can deposit on the filter and later slough off and not be detected when the filter is analyzed. (Cohen & Charles S. McCammon, 2001)

NIOSH NEAT Method

NIOSH has put forth the Nanoparticle Emission Assessment Technique (NEAT) method for characterizing operations that utilize nanoparticles. NEAT is a systematic approach to assessing nanoparticle operations within a workplace. The first steps of the process involve researching the process and an initial walkthrough to gain familiarity with the work process. The next step is to use an OPC and CPC to determine a background concentration of particles with the process off. The process should then be started and OPC and CPC measurements are again taken. At this point, the two readings are compared. If the particles counts are “lower” no further sampling is indicated. When a “higher” reading is encountered further sampling should be performed. The NEAT method recommends side-by-side filter-based air samples, one for Transmission Electron Microscope/Scanning Electron Microscope TEM/SEM analysis and the other for mass-based analysis. Another set of filter-based air samples should also be taken away from the process for comparison. Once the process has been completed, another background measurement with the OPC and CPC should be taken. The NEAT process then suggests subtracting the average background readings from the process-specific measurements that were taken earlier. The NEAT process was presented in the NIOSH approaches to safe

nanotechnology document though was not termed NEAT. Later presentations by NIOSH personnel termed the same process NEAT. (NIOSH, 2009)

After the data collection portion of this study was completed Methner *et al.* published two papers using the NEAT method. The first paper discussed the NEAT process and its development. (Methner, Hodson, & Geraci, 2010) The second paper discussed twelve field studies utilizing the NEAT method. (Methner, Hodson, Dames, & Geraci, 2010)

OPC

Optical Particle Counters (OPC) are a particle detection and counting technology that uses light diffraction and detection to count particles in specific size ranges. Particles pass into the instrument and are then directed one at a time through a light beam. When the particles pass through the light energy is reflected to a detector. The detector converts this reflected light to an electrical signal. The electrical signal strength is used to determine a count and which of the instruments size channels the particle falls within.(Hinds, 1999)

OPCs have several limitations. The major limitations are that the detector can be overwhelmed and that the refracted light is not monotonic for particles sized between 0.5 and 1.5 μm , as well as response error for different refractive indexes of particles. Particle detection is not 100% due to more than one particle passing through the light beam at a time. When more than one particle is in the light beam at a time they can be interpreted as one particle because one particle hides behind another. This coincidence can be overcome by reducing the flow through the detector or diluting the incoming aerosol with

filtered air not containing particles. The monotonic limitation is due to the signal that is returned by the detector not being unique to a particular particle size. That same level of signal is associated with a range of particle sizes. Another limitation is the fact that the instrument loses accuracy when a range of refractive indexes are present. Detector response error ranges from -50-140% depending on the refractive index that is present. (Hinds, 1999)

For this study an AeroTrak 8220 (TSI; Shoreview, MN) will be used. The AeroTrak 8220 has a detection range of 0.300-10 μm . The coincidence loss for the 8220 is 5% for particle concentrations less than 2,000,000/ft³ (70/cc). The 8220 has an accuracy of 50% \pm 10% at 0.300 μm and achieves 100% by 0.45 μm . (TSI, 2006)

CPC

Condensation Particle Counters (CPC) is a particle detection and counting technology that grows particles in a super saturated environment so that they can be more easily counted. Particles are introduced into the instrument and are then sent through a supersaturated isopropyl alcohol solution where they are grown. The exposure time and concentration are both closely controlled and particles are grown to 10 μm in diameter. Particles grow to the same 10 μm size regardless of their original diameter. These 10 μm can now be easily counted via a calibrated light transmission detector. Due to the growth of the particle counts for particles within the detection rang can be performed but particle size cannot be determined. (Hinds, 1999)

CPCs are limited in two ways; they have a maximum concentration of particles that they are able to detect and the inability to differentiate between particles of a

different size. Due to the fact that particles grow to the same diameter regardless of their original diameter the meter is unable to differentiate between particles sizes and only reports a raw particle count/cc measurement. (Hinds, 1999)

For this study the CPC used is a PTrak 8525 ultrafine particle counter (TSI; Shoreview, MN). The 8525 has a particle size detection range of 0 – 1 μm . The particle detection range for the 8525 is 0 – 100,000 particles/cc. (TSI, 2007)

Measurements

With the OPC's limit of detection at a size of 0.3 μm it is not able to detect particles in the nanoscale. The CPC with a limit of detection at a size of 0.01 to 0.02 μm is able to detect particles in the nanoscale but cannot distinguish them from particles in the upper range of its detection limit of 1 μm . NIOSH has stated that a means of overcoming these limitations and building on the strengths of these detectors is to run them in parallel and use the OPC data to determine which portion of the CPC data is below the limit of the OPC. (NIOSH, 2009) Heitbrink *et al.* put forth a method for combining this data. Utilizing the fact that the detectable sizes for the two meters overlap, the size channels of the OPC that are below the 1 μm upper detection limit of the CPC are subtracted from the CPCs count. The remaining value represents particles with diameters below the OPC detection limit of 0.3 μm . Heitbrink *et al.* define this value as the number of ultrafine particles (C_{un}) calculated as shown in equation (1).

$$C_{un} = N_{cpc} - \sum_{i=1}^5 C_{n,i} \quad (1)$$

Where N_{cpc} = the CPC count. The number 5 is the OPC channel for which the upper boundary is $1.0 \mu\text{m}$ for the meter used by Heitbrink *et al.* $C_{n,i}$ is the count returned for the i th channel of the OPC, where i is the OPC channel being summed. (Heitbrink, Evans, Ku, Maynard, Slavin, & Peters, 2009)

Surface Area

As discussed previously, surface area has also been shown to be a possible dose metric for nanoparticles and is one of the three properties that Maynard has recommended being measured when performing evaluations of nanoparticle operations. (Maynard, 2006) Particle surface area can be estimated using measurements of particle size and distribution utilizing the concept of mobility diameters. This is the same technique used for Scanning Mobility Particle Sizers (SMPS). This technique is very complex to execute and therefore expensive as well. An easier method for the measurement of surface area utilizing an Electrical Aerosol Detector (EAD) is put forth by Wilson *et al.* The EAD is based on the concept of diffusion charging where a charge is attached to the surface of an aerosol, measured, and then used to determine surface properties of the aerosol. (Wilson, et al., 2007)

The EAD samples the aerosol and splits the flow into two parts. The first part is sent into a mixing chamber without any change. The second part is sent through activated carbon and high efficiency particulate air (HEPA) filters which are used to clean the air. The clean air is then charged using a corona needle and sent to the mixing chamber. Within the mixing chamber the charged ions attach to the particles that have been sampled. The mixture is then sent through an aerosol electrometer where the current

generated is measured. This current is then related to the amount of surface area of the particles deposited in the lungs. (Wilson, et al., 2007)

The limitations of the EAD include that it may not measure a geometric surface area of the particles in question, but rather the active surface area of the particles. That is, the area that is available for reaction with the environment surrounding the particle. Additionally, the relation of the output of the EAD must take into account the breathing rates of the worker population being evaluated as the output is in units of area per volume. This means workers who are performing administrative tasks will inhale a smaller volume of air than workers who are performing manual labor. (Wilson, et al., 2007)

For this study an AeroTrak 9000 Nanoparticle Aerosol Monitor (TSI; Shoreview, MN) is the EAD that will be used. This AeroTrak 9000 has a particle size detection range of 20-1000 nm with the 1 μm cyclone in place. For the alveolar deposition region the AeroTrak 9000 has a surface area detection range of 1-10,000 $\mu\text{m}^2/\text{cc}$. It has an accuracy of $\pm 20\%$ for particles in the 20-200 nm size range. (TSI, 2006)

Problem Statement

Currently, there is little knowledge on how to control exposure to composite fibers. In fact, one of the reasons for this study is the fact that NIOSH asked if the Air Force had any research or guidance on the control of composite fibers due to a request from the Army. With this lack of knowledge a research plan was developed to add to the body of knowledge on composite fiber exposures by executing a small scale experiment. This experiment will entail the cutting of multiple composite tickets that will have

different controls applied to determine if any of the controls are effective in reducing the exposure. These composite tickets are a 16-ply Bismaleimide (BMI) graphite composite and are representative of the BMI composite material that is used within the F-22 and F-35. (Storage, 2009) Due to the fact that sections of the aircraft will be burnt a set of composite tickets will be burned prior to being cut. The controls that will be evaluated include water as it is readily available at the scene of a crash, wetted water which is water with a surfactant added and is commonly used as an asbestos fiber control, Aqueous Film Forming Foam (AFFF) which is also readily available at the scene due to its use fighting aircraft fires, and a wax solution that is prescribed by the crash response Technical Order. (US Air Force, 2008)

III. Method

Ticket Heat Treatment

Two sets of ACM tickets were prepared for the cut experiments. One set was left intact and a second set was burned before the cuts were made. This is due to the fact that in the event of a crash the aircraft is likely to burn. During this burning process some portions of the aircraft will burn and other portions will be left intact.

To burn the ACM tickets, the tickets were placed in an aluminum container and 100 ml of JP-8 was poured into the container (Figure 1) before JP-8 was added.



Figure 1 ACM ticket burn orientation

JP-8 was used because it is the jet fuel used on Air Force aircraft and would be the most likely fuel for any fire that would occur during an aircraft crash. The JP-8 was then

ignited with a butane lighter and allowed to burn to extinction. A burning ACM ticket can be seen in Figure 2 and a burnt ACM ticket in Figure 3.



Figure 2 Burning ACM ticket



Figure 3 ACM ticket after burn with obvious signs of delamination

The ACM tickets were then removed from the container and placed into a mason jar for storage until the cut experiments were performed. This procedure was repeated for each of the 15 burnt tickets. The burn order was randomized in order to decrease the bias produced by the increased proficiency gained while performing each burn.

Cut experiment

To perform the cuts, a glove bag was setup to prevent exposure to any aerosol generated when the cuts were performed. A ring stand was inserted into the bag as a means of securing the tickets during the cutting process. The DRIs and sample pumps were next to the glove bag as seen in Figure 4.



Figure 4 Experiment setup

To simulate the gas-powered concrete saws commonly used in the field to disassemble aircraft, a dremel tool (Bosch: Farmington Hills, MI) with a cutoff head was selected to cut the ACM tickets. So that the dremel would not be inside the glove bag during the cuts, a dremel tool extension was used as seen in Figure 5.



Figure 5 Dremel tool setup during cut experiments

The use of the extension also eliminated any bias of particles generated by the dremel too. A dremel RPM of 5000 was first selected for the cuts as the concrete saws commonly used to disassemble aircraft operate in the 2500-5000 RPM range. This RPM setting proved to not be practical in cutting intact and burnt composite tickets. At the lower RPM setting the cutoff disk would bog down and would not perform the desired cuts. Due to this fact, a RPM setting of 10,000 was used. A pilot study had shown that this change in RPM would have an effect on the particle size distribution generated by each cut. (Ferreri, Slagley, & Felker, 2009)

For the experiments several gravimetric sample trains and DRIs were used to gather data. For the respirable and total mass samples SKC 50 μg matched weight 37 mm 0.8 μm pore size MCE filters were used. (SKC 225-503; Eighty Four, PA) The

respirable sample train utilized an SKC 37 mm aluminum cyclone to select for respirable sized particles. (SKC 225-01-02; Eighty Four, PA) The OPC used was a TSI AeroTrak 8220. (TSI; Shoreview, MN) The CPC used was a TSI PTrak. (TSI; Shoreview, MN) The surface area meter used was a TSI AeroTrak 9000. (TSI; Shoreview, MN)

The dremel tool extension, respirable mass pump with cyclone, total mass pump, OPC, CPC, surface area meter were then plumbed into the bag as seen in Figure 6.

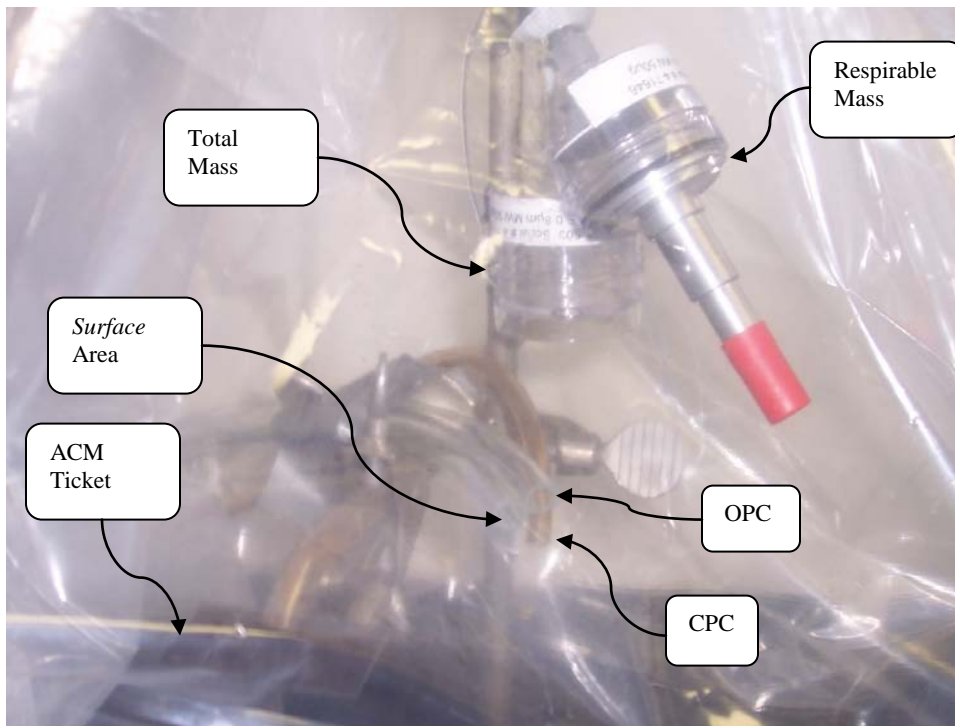


Figure 6 Sampling setup

For each trial the surface area meter and OPC tubing were replaced. This was not possible for the CPC as a specific fitting was required for connection. To prevent bias the CPC tubing was “blown out” using lab air to remove any contamination for the tubing that could alter the results. The CPC was also checked before the next experiment to ensure it read at the previous background levels.

For this study, a baseline of no control and four controls were used on the composite tickets: water, wetted water, acrylic wax solution, and AFFF. The wetted water, also known as amended water within the asbestos community, is simply water with a surfactant added. For this study Cascade Crystal Clear (Proctor & Gamble; Cincinnati, OH) was the surfactant used in a dilution of one part surfactant 150 parts water. This formulation reduced the surface tension of the water so that it would spread on the composite tickets but would not excessively foam. For the wax control, P&G pro line super durable finish wax (Proctor & Gamble; Cincinnati, OH) was mixed 2:1 with water as per TO 00-105E-00. (US Air Force, 2008) The AFFF control was 3M AFFF (3M; St. Paul, MN) and was not diluted. For each of the controls a volume of 8 ml was applied.

The composite tickets were then weighed dry. The tickets then had their control added and were then placed into the glove bag and secured by the ring-stand clamp. Once the glove bag and been sealed the dremel tool was turned on along with the sample pumps and DRIs. A cut approximately 7 mm long was then performed. The DRIs were allowed to finish their one minute samples. Three more 7 mm cuts were then performed so that enough mass would be detected on the respirable sample.

The total mass pump was turned off after approximately two minutes of sample time. A sample time of two minutes was used as the total mass sample to prevent overloading of the filter which would affect accurate weights. The respirable mass pump was allowed to run for approximately 20 minutes so that sufficient mass would be deposited on the filters so that values were above the limit of quantification. Sample cassettes were then removed from the glove bag, disassembled, and weighed. The

cassettes were then reassembled and capped so that further analysis could be performed. The ACM ticket was then removed from the glove bag and weighed dry as the control had evaporated off by this time. The post cut weights for the burnt tickets were not considered reliable as much of the composite fiber had flaked off during the cutting process as seen in Figure 7.



Figure 7 Burnt ticket post cut with obvious flaking off of material due to delamination

The order in which each sample was cut was randomized to reduce any bias generated by the proficiency gained during each cut experiment. Representative respirable samples were then analyzed using an SEM microscope.

Instrument Setup

Surface Area Meter

The surface area meter was set to sample for the alveolar region of the lungs, that is particles that will deposit in the gas exchange region of the lungs (50% cut point of 4 μm)(ACGIH, 2009). Samples ran for one minute in length. The average, maximum, minimum, and time weighted average for this sample were all recorded. The metric used for the surface area meter is the average for the one minute sample.

CPC

The CPC samples were manually started immediately after starting the OPC as shown in the startup order and the meter was manually stopped immediately after the OPC's sample stopped for a sample length of approximately one minute. Initial samples using the CPC produced counts in excess of the 100,000 counts per cc linearity limit for the CPC. To make these values usable, the average value reported by the CPC was multiplied by a coincidence factor calculated by a spreadsheet supplied by TSI. (TSI, 2001) This coincidence factor was originally developed for a Model 3007 CPC but TSI believes that it is applicable to the CPC used in this study. (Brown, 2009) The coincidence factors are not linear and therefore this method likely underestimates the actual concentration as the values above the average would require a greater coincidence factor. Without having the real time data for the meter the best option was to use the coincidence factor that the average concentration would require.

After nine samples it was decided that the number of samples with count averages above the 100,000 count per cc linearity limit was too large. To bring the levels down to

the linear region for the CPC a solution of dilution was selected. The sample air was diluted with “clean” air that had been previously pumped into a tedlar bag. Prior to usage an electronic bubble burette (Sensidyne Gilian Gilibrator-2; Clearwater, FL) was used to determine the dilution factor for the setup. A dilution factor of 5.82 was calculated for the setup that was used for further cut experiments. The average, maximum, and minimum readings for each sample were recorded. The count/cc data was converted to count data by multiplying the count/cc value by the volume sampled by the OPC.

OPC

The OPC was set with the default buckets size ranges of 0.3-0.5 μm , 0.5-0.7 μm , 0.7-1 μm , 1-5 μm , 5-10 μm , and $>10 \mu\text{m}$. The OPC outputted samples as a raw count in each size range. The OPC raw count was recorded for each bucket. The OPC sample time was set for one minute with the standard instrument flow rate of 2.8 LPM (TSI, 2006).

Gravimetric

The gravimetric sample pumps were set at 2.5 lpm and calibrated using standard procedures. The total mass samples were collected with a closed face configuration. Respirable samples had the first cassette section removed and a cyclone was inserted to provide the desired filtration. After the samples were complete the cassettes were disassembled and weighed. The respirable mass filters were weighed first where the “dirty” filter was weighed and then the “clean” filter weighed. Each filter was weighed four times. Once the respirable filters were weighed the identical procedure was repeated for the total mass filters. The mass differential between the average “dirty” filter and

average “clean” filter was then calculated to determine the respirable and total masses. Respirable and total mass concentrations were calculated using the flow rate of the respirable and total mass pumps, the length of time each pump ran, and the calibrated flow rate. After each cassette’s filters were weighed the cassettes were reassembled and capped for future analysis.

SEM Sample prep

Respirable mass filters were chosen to be looked at with the SEM. This is due to the fact that respirable mass will be deposited in the lungs and will not contain the larger particles that are present on the total mass samples. The samples for the SEM had to be prepared. The sample prep had three steps: copper preparation, carbon foil preparation, and sample affixation.

The copper foil (Electron Microscopy Sciences; Hatfield, PA) was cleaned and buffed on both sides to allow for good conductivity for the samples. Once this was accomplished carbon foil was affixed to the copper surface. The carbon fiber samples were then applied to the carbon foil utilizing a razor blade. The razor blade was used to pick up a small sample of the mass collected on the respirable filter. This sample was then set onto the carbon foil. Once on the carbon foil the razor blade was used to spread the sample around so that a thin layer of the sample was present. To make sure the sample was securely affixed to the carbon foil the copper plate was stood on end and tapped after each sample was affixed. This was performed so that no loose carbon fibers or particles were present as they would damage the SEM. The razor blade and forceps

were then cleaned with methanol and the process was repeated for each of these samples. The complete SEM sample prep procedure is located in Appendix B.

Analysis

Once the data was collected a series of averages and standard deviations were completed for each treatment using Microsoft Excel (Microsoft; Redmond, WA). The OPC and CPC data was then used to calculate the Mass Median Diameter (MMD) and Count Median Diameter (CMD) in accordance with Hinds (Hinds, 1999). This was first accomplished with just the OPC data.

In order to combine the data from the OPC and CPC, the fact that the OPC was functioning outside its linearity region had to be corrected for in some way. Three strategies were used to correct for this error in count readings. First the data reported by the OPC was accepted as truth. The second strategy consisted of using the limited coincidence data generated during TSI's development of the OPC used in this study. This data was used to construct a trendline with Microsoft Excel to determine the amount of coincidence at the concentration encountered by the OPC. The trendline produced the equation seen in equation (2) which gives the counting efficiency in percent at the true concentration.

$$\text{Counting Efficiency} = -5.8 * \ln(\text{true count}) + 110.67 \quad (2)$$

The true concentration used was the corrected CPC concentration measured. Use of the CPC as an estimation of the true total count is an underestimation due to the fact that the CPC's detection range has an upper limit of 1 μm . TSI also used CPC concentration for

their testing of the OPC's counting efficiency. Each size bucket was divided by the counting efficiency to provide an estimation of the true particle count in each bucket. The third strategy used to correct for the coincidence as well as the counting efficiency for different size particles. TSI only reports a reduction in counting efficiency on the lower end of the OPCs detection range. O'Shaughnessy and Slagley show that photometer response degrades for both small and large particles. (O'Shaughnessy & Slagley, 2002) Using data presented by O'Shaughnessy and Slagley an estimation of counting efficiency at the midpoint of each size bucket was determined. The value produced by strategy two was then divided by this percentage as well to produce the third estimation of true particle count for each bucket.

The OPC is unable to detect particles smaller than 0.300 μm . In order to calculate a CMD and MMD utilizing particles sizes smaller than 0.3 μm a 0.020-0.300 μm bucket was calculated utilizing the technique used by Heitbrink *et al.* (Heitbrink, Evans, Ku, Maynard, Slavin, & Peters, 2009) Their equation had to be modified as a different OPC with different bucket sizes and widths was used during this study. Equation (3) shows the modified equation used to combine the OPC and CPC count data giving the particle count for the 0.020-0.300 μm bucket.

$$C_{0.020-0.300 \mu\text{m}} = N_{cpc} - \sum_{i=1}^2 C_{n,i} \quad (3)$$

CMD and MMD values were then calculated using the OPC count data and the calculated 0.020-0.300 μm bucket.

Statistics were then performed using analytical statistics software (SAS JMP 8.0; Cary, NC). ANOVA with Tukey's HSD post test was used to determine if any difference between the baseline and any of the four controls existed. The statistical analysis of the data was performed utilizing a number of different metrics for the effectiveness of the controls as a dose metric for nanoparticles has not yet been determined.

IV. Results

A summary of results for the gravimetric samples are shown in Table 2.

Respirable mass concentration data are seen in the “Respirable” column and total mass concentration data are seen in the “Total” column. The data presented is the average of the results of the three trials for each treatment. Each trial had a “dirty” and a “clean” filter. The difference between these weights was averaged and a result for each treatment was calculated. Standard deviations were calculated using the three trials for each treatment.

Table 2 Average respirable and total mass concentration results with standard deviation (mg/m³)

Ticket Status	Control	Respirable (mg/m³)	STDEV	Total (mg/m³)	STDEV
Intact	Nothing	9.08	3.10	276.89	177.83
Intact	Water	11.95	1.80	315.26	27.96
Intact	Wetted Water	13.75	3.70	231.87	62.16
Intact	Wax	9.82	0.91	263.22	45.68
Intact	AFFF	12.50	0.49	405.63	134.51
Burnt	Nothing	13.08	3.62	323.48	21.21
Burnt	Water	9.65	1.92	197.68	60.13
Burnt	Wetted Water	12.72	2.36	241.03	91.03
Burnt	Wax	10.60	6.01	166.91	78.11
Burnt	AFFF	13.41	4.76	226.58	100.77

The respirable fraction was then calculated to determine if any shift in particle mass was caused by the addition of controls. The respirable fraction was used due to the test conditions in which mass removed from the ACM tickets was not repeatable. A summary of the respirable fraction can be seen in Table 3. Results presented are the

averages for each treatment's three trials. The same naming convention used for Table 2 is again used.

Table 3 Respirable fraction averages with standard deviation

Ticket Status	Control	Resp/ Total	STDEV
Intact	Nothing	0.0425	0.03
Intact	Water	0.0384	0.01
Intact	Wetted Water	0.0593	0.00
Intact	Wax	0.0384	0.01
Intact	AFFF	0.0332	0.01
Burnt	Nothing	0.0407	0.01
Burnt	Water	0.0546	0.03
Burnt	Wetted Water	0.0592	0.03
Burnt	Wax	0.0631	0.01
Burnt	AFFF	0.0683	0.04

A summary of results for the CPC can be seen in Table 4. The values reported are the average of the three trials for each treatment. For the CPC, the metric used was the average concentration over the approximately one minute sample. Standard deviations were calculated using each of the three trials for each treatment.

Table 4 Average CPC results with standard deviation (count/cc)

Ticket Status	Control	CPC (count/cc)	STDEV
Intact	Nothing	208482.54	93258.40
Intact	Water	217073.02	44504.32
Intact	Wetted Water	230588.82	51578.23
Intact	Wax	272150.31	50519.68
Intact	AFFF	220926.53	199968.83
Burnt	Nothing	145497.36	50094.23
Burnt	Water	40421.25	42878.96
Burnt	Wetted Water	20541.11	32283.72
Burnt	Wax	133443.85	81216.85
Burnt	AFFF	151876.82	80384.96

A summary of results for the surface area meter can be seen in Table 5. Again, the same naming convention is used. The values reported are the alveolar region deposited surface area as reported by the surface area meter. These values are the average for each treatment over the three trials performed. The result used for the surface area meter is the average surface area over the one minute sample. Standard deviations were calculated using each of the three trials for each treatment. The high average surface area and standard deviations for the burnt wax row are due to one sample with readings well outside the norm for this study. The reading appears to be unreasonable but no legitimate reason could be found to exclude it from the data set.

Table 5 Average surface area meter results with standard deviation ($\mu\text{m}^2/\text{cc}$)

Ticket Status	Control	SAM ($\mu\text{m}^2/\text{cc}$)	STDEV
Intact	Nothing	80.40	39.98
Intact	Water	109.27	28.50
Intact	Wetted Water	142.67	14.94
Intact	Wax	158.75	14.21
Intact	AFFF	73.77	13.62
Burnt	Nothing	75.97	23.90
Burnt	Water	47.41	25.91
Burnt	Wetted Water	30.17	17.77
Burnt	Wax	478.45	731.64
Burnt	AFFF	90.42	13.20

The results for the OPC were returned as counts for each of six discrete size range buckets. Table 6 is the average CMD and MMD value for each treatment calculated using the values for each of the three trials. A density assumption of 2.17 g/cc (NaCl) was used for the calculation of MMD values. NaCl is a common reference aerosol and its density is in line with that of graphite which varies from 2.00-2.25 g/cc (NIOSH, 2005). Carbon fibers are commonly referred to as graphite fiber as the fibers are of graphite. Standard deviations were calculated using each of the three trials for each treatment.

Table 6 Average CMD and MMD values with standard deviation for OPC particle size distribution data (μm)

Ticket Status	Control	CMD (μm)	STDEV	MMD (μm)	STDEV
Intact	Nothing	1.45	0.30	24.61	10.48
Intact	Water	1.48	0.21	25.75	3.89
Intact	Wetted Water	1.62	0.42	20.20	2.23
Intact	Wax	1.57	0.06	21.98	1.46
Intact	AFFF	1.23	0.32	19.17	6.57
Burnt	Nothing	1.51	0.11	20.96	10.98
Burnt	Water	1.31	0.12	13.33	7.86
Burnt	Wetted Water	1.52	0.14	7.70	2.22
Burnt	Wax	1.43	0.23	10.38	3.42
Burnt	AFFF	1.74	0.27	12.95	6.81

CMD and MMD values were also calculated for each of the strategies for combining the CPC and OPC count data. Table 7 shows CMD and MMD values using both the CPC and OPC data accepting the OPC output (strategy 1). Standard deviations were calculated using each treatment's three trials.

Table 7 CMD and MMD using both OPC and CPC with strategy one (μm)

Ticket Status	Control	CMD (μm)	STDEV	MMD (μm)	STDEV
Intact	Nothing	0.1623	0.0007	0.1818	0.0074
Intact	Water	0.1621	0.0002	0.1795	0.0027
Intact	Wetted Water	0.1623	0.0007	0.1824	0.0089
Intact	Wax	0.1620	0.0004	0.1792	0.0041
Intact	AFFF	0.1618	0.0015	0.1764	0.0153
Burnt	Nothing	0.1634	0.0005	0.1929	0.0047
Burnt	Water	0.2542	0.1464	7.7950	13.0453
Burnt	Wetted Water	0.4703	0.3681	24.2925	27.2999
Burnt	Wax	0.1651	0.0031	0.2079	0.0302
Burnt	AFFF	0.1659	0.0037	0.2222	0.0437

Table 8 shows the CMD and MMD values using the both the OPC and CPC data utilizing the trendline to correct for OPC coincidence (strategy 2). Standard deviations were calculated using each treatment's three trials.

Table 8 CMD and MMD using both OPC and CPC with strategy two (μm)

Ticket Status	Control	CMD (μm)	STDEV	MMD (μm)	STDEV
Intact	Nothing	0.1658	0.0014	0.2188	0.0189
Intact	Water	0.1653	0.0006	0.2134	0.0096
Intact	Wetted Water	0.1659	0.0016	0.2223	0.0242
Intact	Wax	0.1653	0.0009	0.2143	0.0107
Intact	AFFF	0.1644	0.0036	0.2036	0.0412
Burnt	Nothing	0.1682	0.0009	0.2473	0.0103
Burnt	Water	0.2923	0.1948	10.7540	17.8864
Burnt	Wetted Water	0.5449	0.4164	25.7160	22.0979
Burnt	Wax	0.1714	0.0058	0.2837	0.0698
Burnt	AFFF	0.1735	0.0075	0.3365	0.1235

Table 9 shows the CMD and MMD using both the OPC and CPC values with both the trendline and particle size OPC coincidence corrections (strategy 3). The burnt wetted water and burnt water MMD results are outside of the norm due to very large geometric standard deviations (GSDs). The Hinds method of calculating MMD is very sensitive to GSDs over 3 as in this case. The large MMD values are a function of mathematics not reality. These treatments had large GSDs due to the low CPC values presented earlier.

Table 9 CMD and MMD using both OPC and CPC with strategy three (μm)

Ticket Status	Control	CMD (μm)	STDEV	MMD (μm)	STDEV
Intact	Nothing	0.1706	0.0056	0.3144	0.1234
Intact	Water	0.1714	0.0019	0.3211	0.0447
Intact	Wetted Water	0.1726	0.0042	0.3489	0.0977
Intact	Wax	0.1712	0.0018	0.3138	0.0329
Intact	AFFF	0.1690	0.0075	0.2861	0.1317
Burnt	Nothing	0.1767	0.0027	0.4214	0.0748
Burnt	Water	0.3638	0.2918	30.6314	51.4122
Burnt	Wetted Water	0.7174	0.5793	61.9463	55.2185
Burnt	Wax	0.1796	0.0082	0.4491	0.1461
Burnt	AFFF	0.1857	0.0128	0.7088	0.4035

SEM images were also taken of a number of samples. Figure 8 shows a typical view of a carbon foil with sample attached on the copper plate. In this case, the burnt wetted water sample is in view with the edge of the burnt water sample viewable in the upper right of the image.

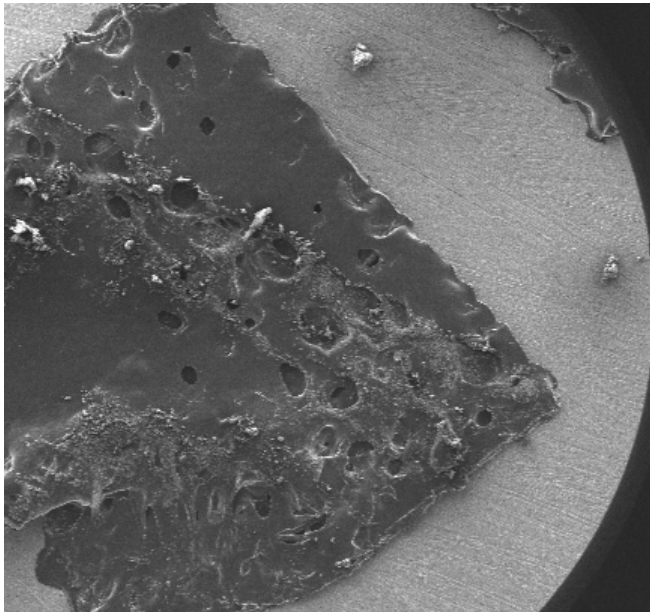


Figure 8 Typical wide view of carbon foil with sample (burnt ACM with a wetted water control)

Figure 9 shows a partially decomposed fiber from a sample of intact ACM with no control applied. The intact fiber can be seen on the right with remnants of the fiber viewable to the left.

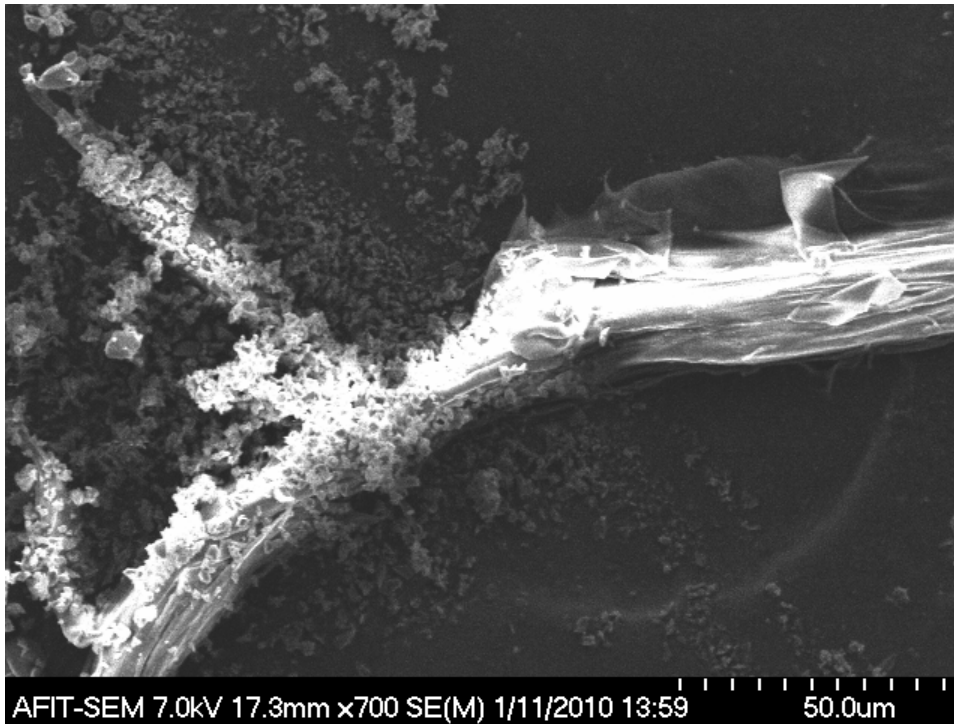


Figure 9 Partially decomposed carbon fiber from an intact ACM sample with no control

Figure 10 shows two carbon fibers overlapping with one fiber showing signs of sample decomposition. This image is from an intact ACM sample with a wetted water control.

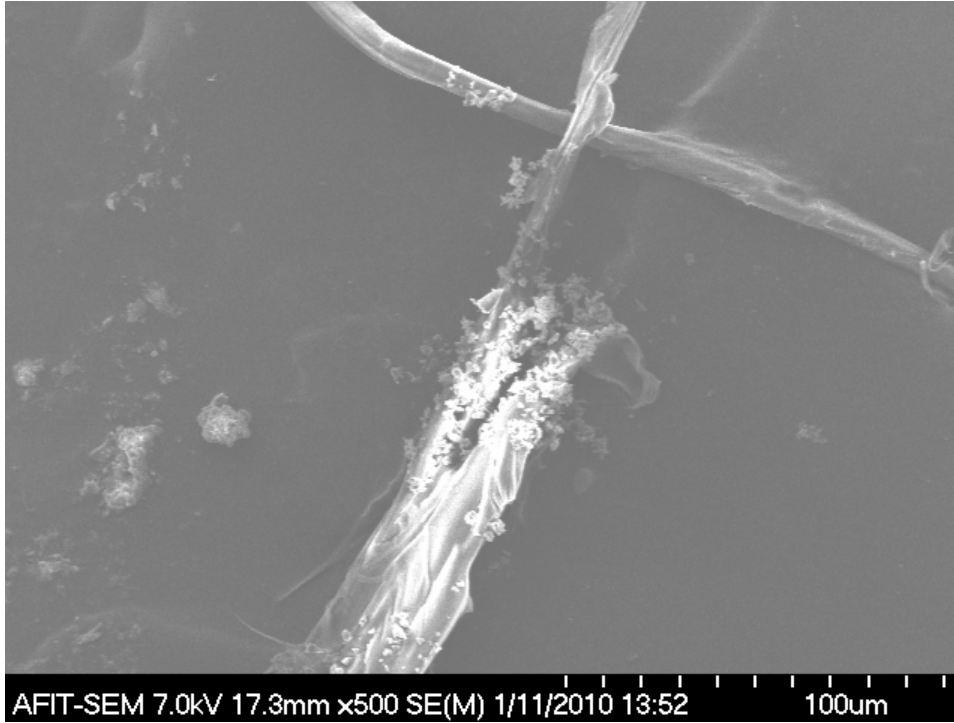


Figure 10 Overlapping partially decomposed carbon fibers from an intact ACM sample with a wetted water control

Figure 11 shows a larger carbon fiber with a filament protruding to the right. The image is from a burnt ACM sample with no control applied.

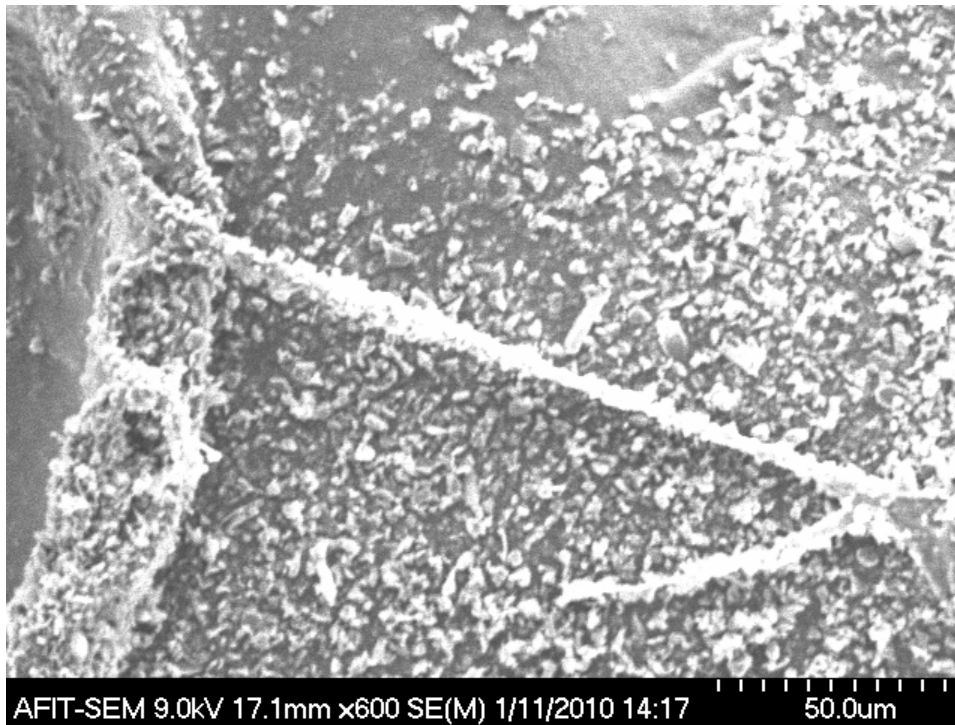


Figure 11 Carbon fiber with filament attached from a burnt ACM sample with no control

Figure 12 shows a close-up of the filament seen in Figure 11 so the size could be determined. The width of this fiber appears to be on the order of 3.5 μm .

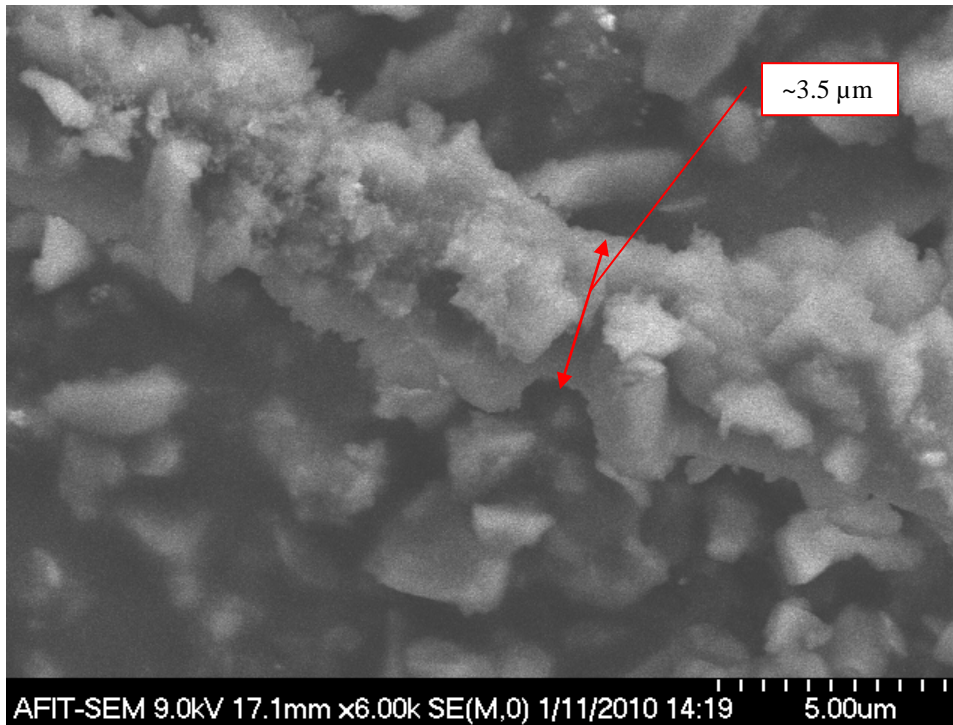


Figure 12 Close-up of filament from a burnt ACM sample with no control

Figure 13 shows a close-up of a particle with a smaller particle on its surface. The smaller particle has a width on the order of 1 μm . This image was taken from an intact ACM sample with a wetted water control.

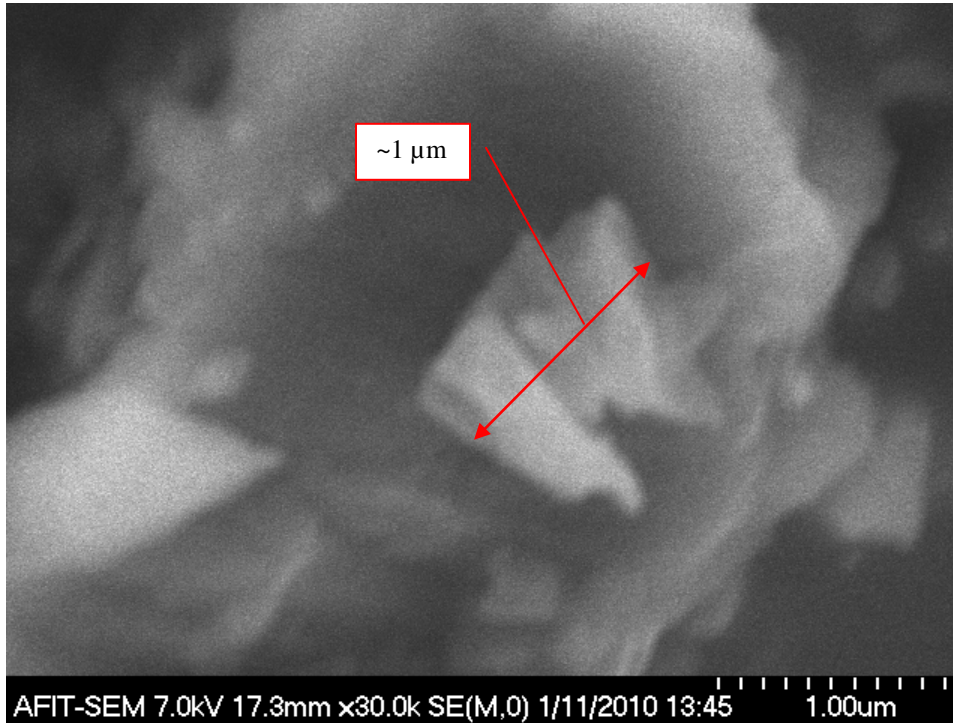


Figure 13 Close-up view of fiber with particle attached

Figure 14 shows a particle with submicron filaments protruding from its surface. This image was taken from a burnt ACM sample with a wetted water control.

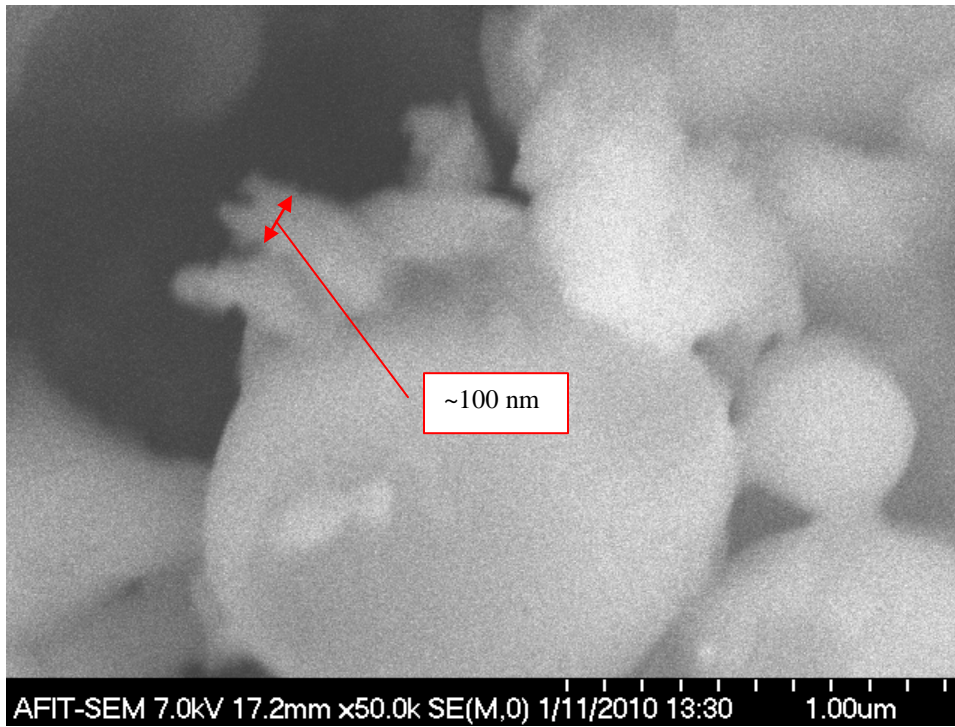


Figure 14 Carbon particle with sub micron filament protruding (burnt ACM with a wetted water control)

V. Discussion/Conclusions

Introduction

The purpose of this study was to test different particle control methods for both burnt and intact ACM samples. The metrics used to compare the effectiveness of these controls were not simply gravimetric (total and respirable mass concentration), but also particle size (CMD and respirable fraction) and surface area.

Intact Tickets

The intact ticket metrics were all compared to the baseline of no control applied to the tickets prior to the cuts. This was done to determine if the pretreatment controls provided a benefit when compared to no control applied to the ACM tickets. To accomplish this, a number of metrics were used to evaluate the different control's effectiveness. The metrics used were: respirable mass, total mass, respirable mass fraction, surface area, CPC concentration, OPC CMD, OPC MMD, OPC+CPC CMD, and OPC+CPC MMD.

There was no statistical difference found for either the respirable mass concentration or the total mass concentration air samples that were taken. F-values were 0.16 and 0.37 respectively. The respirable fraction was also evaluated to determine if any of the controls shifted the mass out of the respirable fraction so that it would present less of a hazard. No statistical difference was found for the respirable fraction as well. The F-value was 0.74.

The surface area meter did show statistical difference for the samples with an F-value of 0.0061. Due to this, Tukey's HSD post test was performed to determine which of the controls performed best. The test produced a grouping of statistical difference as shown in Figure 15.

Level	Mean
Wax A	158.74667
WW A B	142.67333
W A B C	109.26667
N B C	80.39667
AFFF C	73.76667

Levels not connected by same letter are significantly different.

Figure 15 JMP 8.0 Tukey's HSD post test grouping for surface area monitor

As shown in the output, the baseline of no control and the AFFF control performed best. The wax control and wetted water control performed worst. No obvious reason for this difference is apparent. The difference is likely based on the aerosolization of the wetting agent in the wetted water as well as the wax in the wax control. The surface area monitor likely counted these droplets.

The particle counter DRIs were then evaluated. The CPC outputs of particle concentration were not statistically different with an F-value of 0.95. The OPC outputs were used to generate CMD and MMD values. Neither the CMD nor MMD values showed any statistical difference. The F-values were 0.53 and 0.62 respectively.

The OPC and CPC values were then combined and used to calculate another set of CMD and MMD values. None of the OPC+CPC CMD or MMD values showed any statistical difference. The F-values for strategy one were 0.93 and 0.92 respectively. The

F-values for strategy two were 0.88 and 0.89 respectively. The F-values for strategy three were 0.91 and 0.95 respectively.

The pretreatment controls showed little effectiveness for intact tickets. None of the controls showed any reduction in mass concentration, surface area, or particle concentration. Additionally, the controls showed no statistically significant shift in the particle size distribution.

Burnt Tickets

As with the intact tickets, the burnt ticket metrics were all compared to a baseline of no control applied to the tickets prior to the cuts. This was done to determine if any of the pretreatment controls provided a benefit when compared to nothing applied to the ACM tickets. To accomplish this, a number of metrics were used to compare the different controls. The metrics used were the same as the intact tickets.

The respirable mass concentration and the total mass concentration samples showed no statistical difference. The F-values were 0.72 and 0.20 respectively. For the total mass samples, while not statistically significant, the wax control did show some signs of benefit. This is likely due to the fact that the wax acted as an adhesive holding the larger particles together causing them to precipitate before they could be sampled. The respirable fractions were then evaluated and no statistical difference was found. The F-value was 0.74.

The surface area meter showed no statistical difference for any of the controls. The F-value was 0.45. The DRI particle counters were then evaluated. While not

statistically significant the water and wetted water controls showed some benefit for the CPC particle concentration measurement as seen in Figure 16.

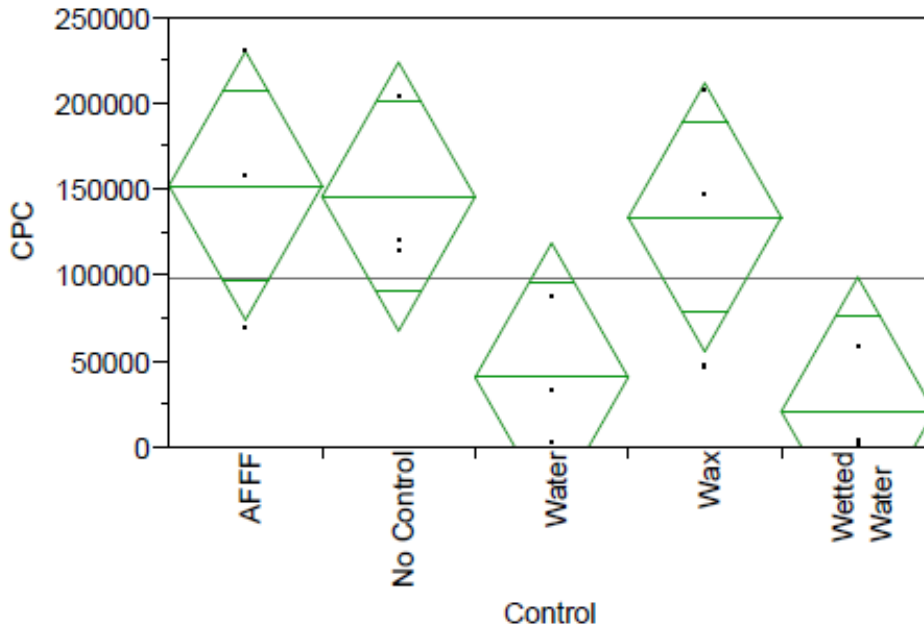


Figure 16 JMP 8.0 ANOVA of CPC count/cc metric for burnt tickets

The F-value for this case was 0.062. It was observed during water and wetted water control application that on the intact sections of the burnt tickets water would bead up but beads were not visible on the burnt sections of the ticket. Similarly, for wetted water applications a film of water was visible on the intact sections of the ticket whereas no such film of water was visible on the burnt sections of the ticket.

The OPC CMD and MMD values were then evaluated. Neither the CMD nor the MMD showed statistically significant difference. The F-values were 0.14 and 0.27 respectively. The low F-value for the CMD was an evaluation of the potential difference between the water and AFFF controls not with the no control baseline.

The OPC and CPC values were then combined and used to calculate another set of CMD and MMD values. None of the OPC+CPC CMD or MMD values showed any statistical difference. The F-values for strategy one were 0.23 and 0.21 respectively. The F-values for strategy two were 0.19 and 0.13 respectively. The F-values for strategy three were 0.18 and 0.17 respectively. While not statistically significant each of the three strategies showed some benefit to the water and wetted water controls. This benefit manifests in a shift of the particle size distribution toward larger sizes.

The wax control did have some effect on the total mass measurement but not for the other metrics that were recorded. This could be due to the fact that the wax adhered the larger particles together so they would precipitate and not be collected by the total mass sampler. These large particles would not be detected by the respirable mass measurement as the cyclone would have filtered them out. The CPC would have similarly not been able to detect the difference in the count of more massive particles due to the upper detection limit of 1 μm . Also, reduction in the count of relatively massive but few in number particles would not significantly affect the surface area or OPC measurements. The water and wetted water controls also showed some effectiveness in reduction of particles in the detection range of the CPC.

Overall Impressions

Due to the variation in the mass removed from the tickets several of these measures have an added level of variation. The measures that are not affected by this variation in mass generation are the respirable fraction, CMD, and MMD. The MMD is determined by a factor multiplied by the CMD. As presented earlier, the MMD showed a

great deal of sensitivity to the high GSDs driven by the particle size distributions of several of the trials. Due to this, the CMD and respirable fraction are the best single measures that are not affected by the difference in mass removed by the cuts. The ANOVA tables for burnt and intact ticket's CMDs using both the OPC and CPC data utilizing strategy 3 can be seen in Figure 17 and Figure 18. The ANOVA tables for the burnt and intact ticket's respirable fractions can be seen in Figure 19 and Figure 20.

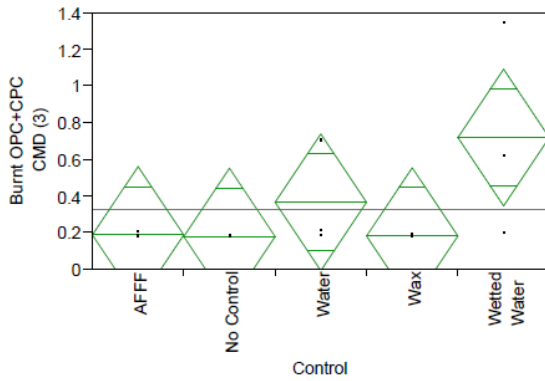


Figure 17 Burnt OPC+CPC CMD using strategy 3 ANOVA table

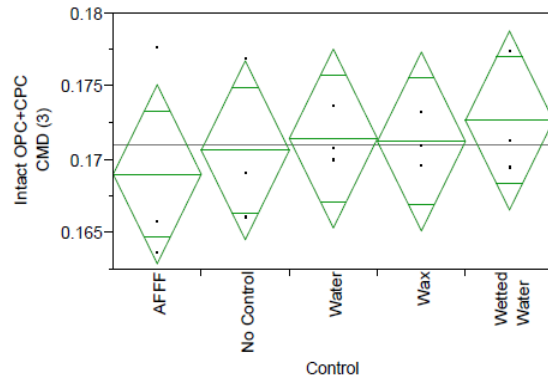


Figure 18 Intact OPC+CPC CMD using strategy 3 ANOVA table

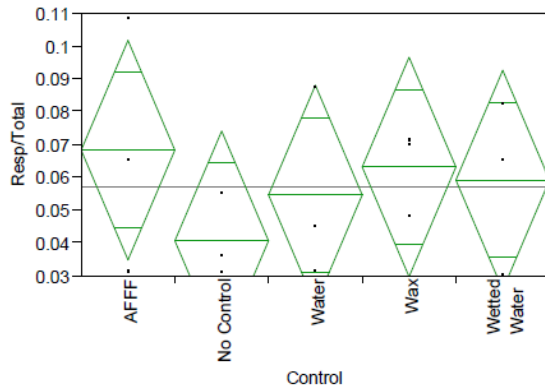


Figure 19 Burnt respirable fraction ANOVA table

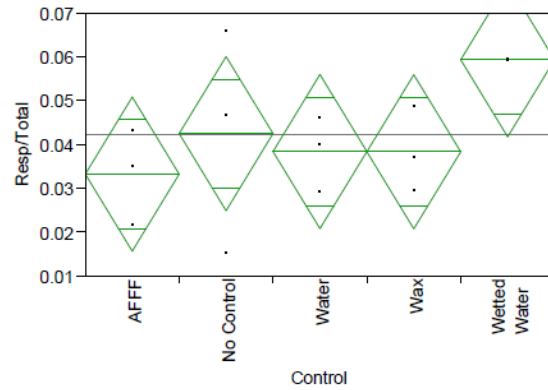


Figure 20 Intact respirable fraction ANOVA table

The CMD for the water and wetted water control did show some improvement when compared to the baseline of no control, though this difference was not statistically significant when comparing the CMD values.

Idealized Particle Size Distribution

To better show the effect of this difference, the arithmetic average CMD and the average geometric standard deviation (GSD) for the particle size distributions over the three trials for each control was calculated. With these CMDs and GSDs, an idealized plot of the particle size distribution curve for each control was plotted along with the theoretical Most Penetrating Particle Size (MPPS) in classical filtration theory of $0.3 \mu\text{m}$ as shown in Figure 21 (Hinds, 1999).

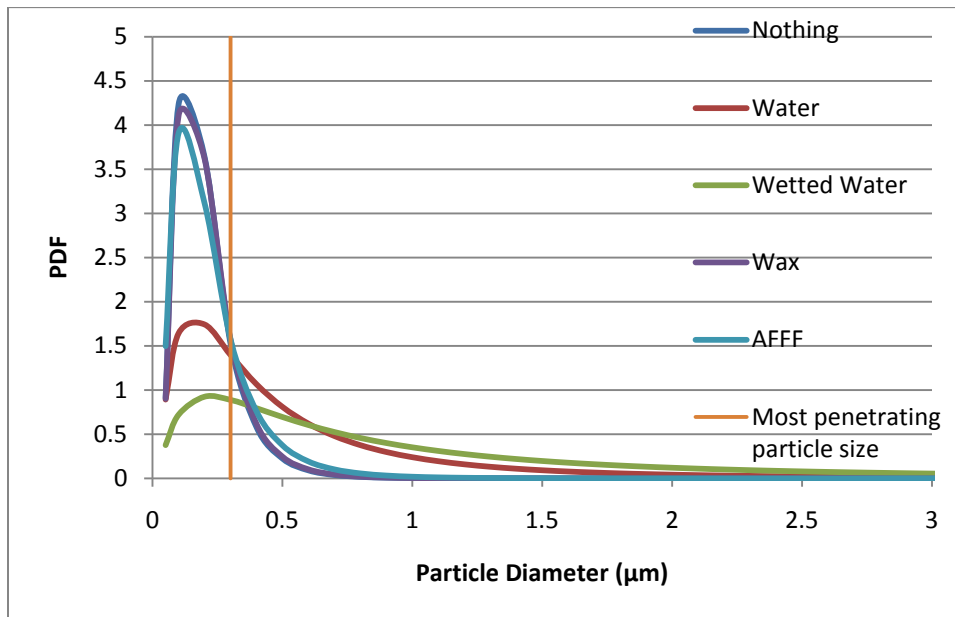


Figure 21 Plot of idealized particle size distributions for burnt tickets based on CMD and CMD GSD (strategy 3) for different control options

While there was not a statistically significant shift in the CMD there is a definite shift in the particle size distribution when the GSD is also taken into account. This particle size distribution shift is relevant due to the use of respirators at the crash site during aircraft disassembly. Similar plots for strategies one and two for the burnt tickets and all three strategies for the intact tickets can be found in Appendix C.

Further, Eninger *et al.* showed that the actual MPPS may be smaller than $0.3 \mu\text{m}$ when utilizing electrets filters (Eninger, Honda, Reponen, McKay, & Grinshpun, 2008). Additionally, Eninger *et al.* showed that the current NIOSH respirator filter testing procedure is not capable of detecting particles $<0.1 \mu\text{m}$ in diameter and particles between 0.1 and $0.2 \mu\text{m}$ in diameter contribute little to the certification metric. (Eninger, Honda, Reponen, McKay, & Grinshpun, 2008) Due to these findings any shift in particle size distribution to larger sizes would reduce the level of aerosol in the more penetrating size range for the respirator filters, thereby increasing the respirator's effectiveness at filtering the aerosol out of the air. This would increase the protection afforded crash recovery personnel utilizing respirators during aircraft disassembly.

To determine if a statistically significant difference existed between the distribution curves a Monte Carlo simulation was run using the natural logarithm of the CMD and GSD to develop sets of data points for each idealized distribution with more statistical power. ANOVA analysis was then performed on each of these sets of normalized data points. A statistically significant difference was found (F-value < 0.0001). Figure 22 shows the ANOVA table. Tukey's HSD post test was then run to determine the order and groupings of the data. Figure 23 shows the grouping generated by Tukey's HSD post test.

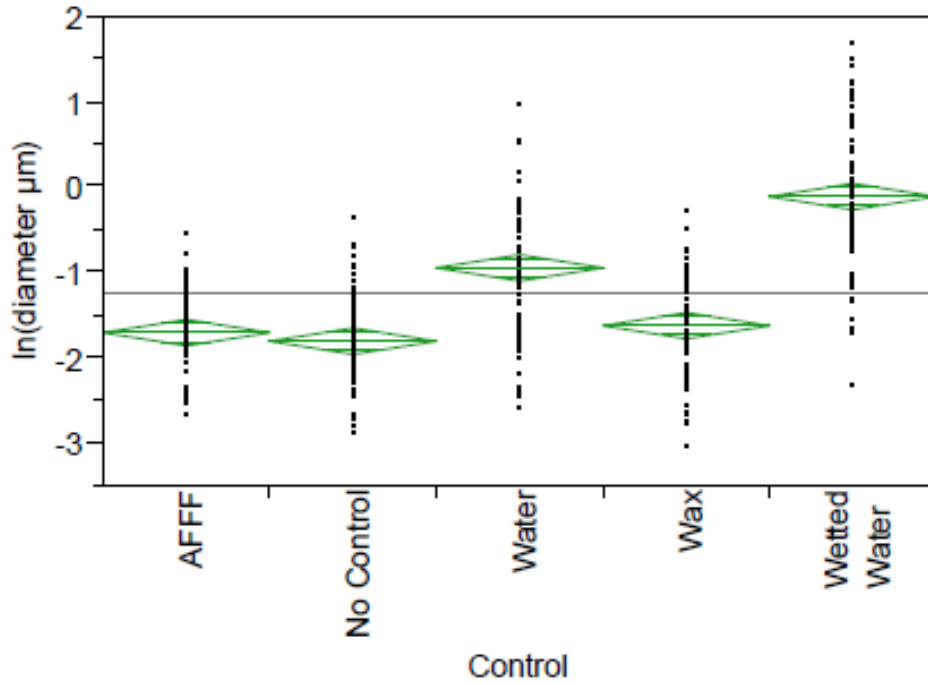


Figure 22 Idealized particle size distribution ANOVA table

Level	Mean
Wetted Water A	-0.116300
Water B	-0.953369
Wax C	-1.631481
AFFF C	-1.713532
No Control C	-1.812994

Levels not connected by same letter are significantly different.

Figure 23 Tukey's HSD grouping of idealized particle size distributions

Respirable Fraction

Due to the overloading of the total mass filters the total mass pump had to be turned off after two minutes of sampling while the respirable mass pump ran for 20 minutes to assure enough mass was collected. To determine if this difference would

affect the gravimetric samples a settling velocity analysis was performed. The terminal settling velocity for a number particle sizes was calculated with equation (4).

$$V_{TS} = \frac{\rho * d^2 * g * C}{18 * \mu} \quad (4)$$

With these velocities, settling distances were calculated at 2, 5, 10, 15, and 20 minutes after start of sampling. The glove bag was supported internally by a 53 cm ring stand. The gravimetric samplers were located at a height of approximately 35 cm. Table 10 shows the calculated settling distances for a range of particles sizes applicable to this study.

Table 10 Settling distances at 2, 5, 10, 15, and 20 minute marks for multiple particle diameters

Diameter (μm)	V _{TS} (cm/s)	2 min (cm)	5 min (cm)	10 min (cm)	15 min (cm)	20 min (cm)
1	0.00751	0.45	1.80	4.05	6.31	8.56
2	0.02787	1.67	6.69	15.05	23.41	31.77
3	0.06109	3.67	14.66	32.99	51.31	69.64
4	0.10716	6.43	25.72	57.87	90.01	122.16
5	0.16615	9.97	39.88	89.72	139.57	189.41
6	0.23787	14.27	57.09	128.45	199.81	271.17
7	0.32250	19.35	77.40	174.15	270.90	367.65
8	0.42000	25.20	100.80	226.80	352.80	478.79
9	0.53051	31.83	127.32	286.48	445.63	604.79
10	0.64274	38.56	154.26	347.08	539.91	732.73
11	0.77772	46.66	186.65	419.97	653.29	886.60
12	0.92555	55.53	222.13	499.80	777.46	1055.13
13	1.08624	65.17	260.70	586.57	912.44	1238.31
14	1.25978	75.59	302.35	680.28	1058.21	1436.15
15	1.44618	86.77	347.08	780.93	1214.79	1648.64

The settling distances were calculated at +1, +4, +9, +14, and +19 minutes due to the fact that the last cuts were performed 1 minute into the sample time. Additionally, Cunningham slip correction factors were used for particles less than 10 μm in diameter.

A decision point of a settling distance greater than the bag height was used to determine if the particle size would settle out of the sample environment. Due to the fact that the respirable pump used a cyclone to select for particles in the respirable fraction some of the particles that settled out would not affect the respirable mass as they are outside of the respirable fraction. Table 11 shows the settling threshold calculated at each time hack, that is particle with larger diameters than indicated will have settled by the time hack.

Table 11 Settling threshold at 5 time hacks

Time	2 min	5 min	10 min	15 min	20 min
Diameter (μm)	11.75	5.77	3.8	3.05	2.59

Figure 24 overlays the respirable fraction curve with the settling diameter at time hacks of 2, 5, 10, 15, and 20 minutes. At these time hacks only particles with diameters smaller than indicated will be available for collection on the respirable filter, and only a fraction of them will still be aloft.

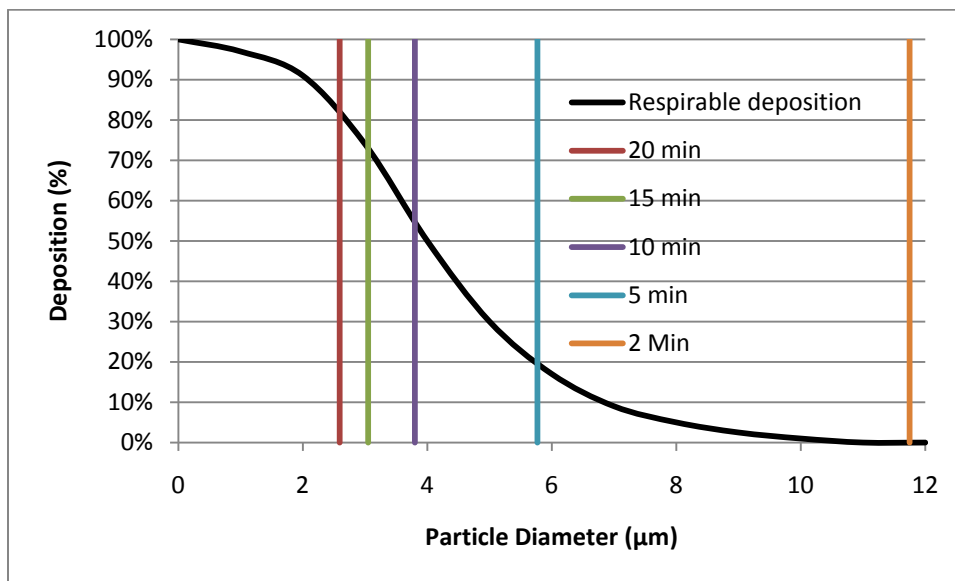


Figure 24 Respirable deposition percentage along with settling size a 5 time hacks

To determine if this settling effect would alter that data an analysis of the particle size distribution was conducted. Using the particle size distribution data an estimation of what percentage of the mass present at the one minute mark (active cutting) was available at the 2, 5, 10, 15, and 20 minutes marks. This analysis assumed a density of 2.17 g/cc (NaCl) for the particles and spherical particles of the dimension detected. The vast majority of the mass available for collection was airborne during the first minutes of sampling (first cut) as well as the early part of the second minute (remaining cuts) while both the total mass and respirable mass pumps were active. Table 12 shows the percentage of the original mass that is aloft 2, 5, 10, 15, and 20 minutes into the sampling.

Table 12 Percent of original mass aloft at 5 time hacks

Time	2 min	5 min	10 min	15 min	20 min
Mass left aloft (%)	81	22	08	04	03

The mass available for collection decreases as time passes due to the settling of the more massive large diameter particles. Due to this fact, if the total mass sampler would have continued sampling past the two minute mark it would have added decreasing amounts of mass as time passed.

An analysis was attempted that determined what the total mass filter would have weight had it sampled 20 minutes but the mass concentration derived from the particle size distribution data was more than an order of magnitude greater than the mass collected on the total mass filters. This difference is likely due to the assumptions that optical diameters detected constituted spherical particles of that size. Such an assumption would over estimate the volume of the particles detected as a sphere would be the largest

possible volume associated with a given optical diameter. The actual volume of the particle would likely have been much less and hence its mass would have been less. Additionally, the density assumption of NaCl may not be accurate due to the nature of the fibers and the binder present in the ACM panels.

Water

The water control showed some benefit for the burnt ACM tickets where the CPC showed lower particle concentrations. This benefit was not statistically significant but was noticeable. Water also showed obvious but not statistically significant benefit for the shift of the idealized particle size distribution. The water control showed no effect for the other metrics used in this study. The water showed no benefit for the intact ACM tickets.

Wetted Water

Wetted water showed a statistically significant shift in the particle size distribution of the idealized particle size distribution. Similar to the water control, the wetted water also showed some benefit for the burnt tickets where the CPC showed lower particle concentrations. This benefit was not statistically significant but was noticeable.

Wax

The wax control that is recommended by the crash response TO showed benefit only for the burnt total mass concentration samples. As discussed earlier, this is likely due to the precipitation of the larger mass particles before they were collected by the sampler. This precipitation effect would also prevent inhalation exposure. The wax showed no statistically significant benefit for the other metrics used in this study. This study did not evaluate the ability of the wax to act as a fixant for particles that have been

previously released during cutting or the fire itself. Further evaluation will be needed to determine if the wax is effective at controlling carbon fiber particulate during inspection of the crash as well as the packaging and handling of the aircraft components.

AFFF

The AFFF showed no statistically significant benefit for any of the metrics used in this study for burnt or intact tickets. This may be due to the foaming nature of the AFFF. That is, the AFFF is designed to reduce the surface tension of the water in which it is added to produce foam which prevents oxygen from reaching a fire. This foaming may not allow for the AFFF to help agglomerate the particles as they are cut away from the ACM tickets. However, the same effect was not present for the wetted water control where a reduction in surface tension did allow for the control of particles. The cause of the wetted water's control of the aerosol and AFFF's lack of control is unknown. While an effective fire fighting agent, AFFF should not be relied upon to control carbon fiber particulates.

SEM

The SEM images showed a number of significant features. Fibers were observed in both the burnt and intact tickets. This would indicate that fibers can be released when intact ACM panels are cut. This is of interest due to the fact that with the large number of ACM panels within the Air Force inventory maintenance work will be needed. These ACM panels will have damaged sections removed so that replacement panels can be put into place. (US Air Force, 2007) The fiber filament seen in Figure 11 and Figure 12 show that the fibers will reduced in size as part of their oxidation and fibrillation as was

shown in the NASA study. Due to the sample preparation technique it is likely that a number of fibers were broken apart. Less destructive SEM sampling techniques may show more fibers of similar size and TEM images would have the ability to show fibers in the submicron scale.

The SEM images also showed a number of particles in the 1 μm size range. Particles in this size range were generated cutting both the intact and the burnt samples. No discernable differences in the particles were seen between burnt or intact ACM tickets. This could be due to a true lack of difference or the transfer technique that was used. These particles appear to have a number of jagged edges and protrusions and do not meet the fiber definition of having an aspect ratio of 3:1. The particle shown in Figure 14 shows a protrusion on the order of 100 nm. These protrusions fall into the definition of nanomaterials. This would be a nanostructured material as described by Maynard and Kuempel. (Maynard & Kuempel, 2005) Nanostructured materials may act similarly to true nanomaterials when they interact with the body. This is due to the fact that the nanostructure will have the same properties as a nanomaterial as perceived by the body tissue that it is interacting with even though it is part of a large micron size particle.

Pretreatment Effectiveness

The pretreatment controls were shown to be effective at shifting the particle size distribution toward larger sizes. The use of pretreatment controls did not eliminate or reduce the need for respiratory protection. However, the pretreatment controls showed limited effectiveness in the reduction of potential exposure as measured in this study.

This is likely due to the amount of energy the blade imparted to the particles as they were removed from the ACM tickets.

The water, wetted water, and wax controls showed more effectiveness on the burnt tickets than the intact tickets. One likely cause of this lack of effectiveness on the intact tickets is the amount of interaction between the control and the blade as it cut the ACM ticket. Figure 25 shows a depiction of the interaction area of the control and the cutting blade.

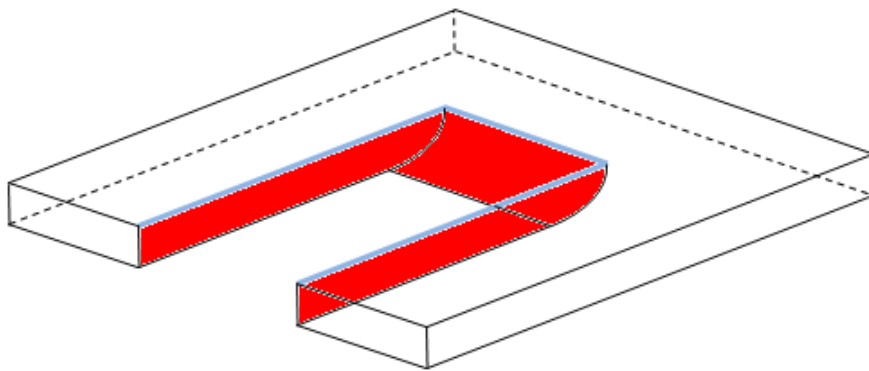


Figure 25 Diagram of interaction area of blade and control for intact tickets (blue) as compared to interaction of blade and burnt tickets (red)

The blue highlighted line is the site where the blade will interact with the control when cutting an intact ticket as the control will sit on top of the ticket. This area is far less than the area where the blade is interacting with the burnt ticket shaded in red. The larger burnt interaction area is due to the delamination of the carbon fibers allowing the controls to soak into the ACM ticket to some degree allowing for more interaction with the blade.

Potential Controls

While this study did show a shift in the particle size distribution, it did not show any statistically significant reduction in any of the exposure metrics used. The next step

in the control of these particles would be some type of active control during the cutting process. In the construction industry the use of concrete saws presents a number of airborne hazards, most notably quartz and silica exposure. Due to this, several attempts have been made to control the dust generated by concrete saws. Nij *et al.* showed that Local Exhaust Ventilation (LEV) and cooling water controls for concrete saws can reduce quartz exposures by at least 80%. (Nij, et al., 2003) Such LEV or wet method controls would likely reduce the level of particle aerosolization when similar concrete saws are used to cut ACM panels. Middaugh showed similar reductions for silica of 87.7% and 87.0% for wet saw methods and LEV respectively when compared with dry methods in a thesis conducted at Purdue University. (Middaugh, 2009)

Sampling Methodology Improvements

This study evaluated the usage of several pretreatment controls to determine if there was a reduction in potential exposure during the cutting of carbon fiber composites. Another purpose of this study was to determine effective means of sampling carbon fiber processes. With this in mind, several improvements to the sampling methodology used in this study could be made to more precisely evaluate airborne exposure to carbon fiber composites during cutting or other operations. The cutting of the composite tickets was not well controlled or repeatable during this study. During future small scale experiments a jig should be constructed that would allow for the precise control of roll and yaw of the blade as well as the cut length. The usage of a jig would reduce the variation in the amount of material that is cut from the tickets and eliminate a potential cause of measurement variation. This variation in the amount of material cut due to blade

orientation would not be significant if a concrete saw were used. This is due to the fact that the cut would be much longer and any variation in the roll angle of the blade would not significantly alter the total amount of material removed from the ACM panel.

If gravimetric samples are taken in future studies dedicated gravimetric media should be used. When this study was started, analysis for the samples for fibers was anticipated and therefore MCE media was used. Preweighed PVC media should be used for any future gravimetric samples due to PVC media's lack of sensitivity to humidity. Additionally, particle settling should be taken into account if respirable fractions are calculated. The most desirable remedy would be longer cut times due to the fact that the generation of particles is the exposure of interest not the exposure to particles some period of time after generation. A series of consecutive total mass samples could be used to prevent filter overload while the respirable sample continued to run until sufficient mass was collected on the filter. This remedy would prevent different particle size distributions being sampled by the two gravimetric samplers and would more closely evaluate the exposure due to cutting an ACM panel.

Another potential metric for carbon fiber sampling is NIOSH method 5040. While a useful academic exercise, the gravimetric sampling adds several levels of variation to the measurement of the carbon fibers and carbon fiber particulates as part of the sampling procedure. Gravimetric sampling is insensitive to changes in the amount of very light particles that were of concern in this study. Gravimetric sampling also gives no indication of the nature of the matter that is collected, only its mass. NIOSH method 5040 is designed for diesel particulate but actually samples elemental carbon using a

Flame Ionization Detector (FID). (NIOSH, 2003) The NIOSH NEAT technique uses this method as an indication of the presence of CNT during sampling.

The SEM transfer methodology used in this study did not allow for many conclusions to be drawn from the images that were produced. Due to the limitations imposed by the SEM that was available for analysis great care needed to be taken to prevent loose particles from being present on the sample. Due to this, the samples had to be continuously tapped to “shake off” any loose material. This process would likely remove any particles that were only loosely bound to the carbon foil and prevent the detection of submicron particles. Also, this tapping would also contribute to the breakup of any fibers that were present on the media. Future studies should use a dedicated lab that is familiar with SEM or more desirably TEM analysis. TEM analysis would provide the ability to take images with greater magnification. Filters could be specifically sampled for this type of analysis and sent to the lab where the filter could be dissolved onto the appropriate media and then analyzed. Such a procedure would provide the ability to detect nanomaterials and also allow for conclusions to be drawn from the morphologies that were present on the filters.

The TSI OPC used in this study was not reliable at the particle concentrations encountered. The upper limit for the linear region for the OPC was 2,000,000 counts per cubic foot (70 counts/cc), which is remarkably low. The CPC used in this study measured the background level of particulate in the air as 300-500 counts per cc. Due to the level of aerosol generated in this study dilution was necessary to keep particle concentration levels below 100,000/cc for the CPC. A similar dilution setup would not have been possible or practical even if attempted for the OPC. A dilution factor of 1428

would have been required to reduce a value of 100,000 to the linear region of the TSI OPC. Concentration values observed in this study were often much higher than this value. Such a dilution setup would have reduced the fidelity of the OPC readings a great deal and potentially reduced the OPC's usefulness. Future studies looking at composite fibers should use a different OPC such as the Grimm OPC which has a saturation level of 100,000 counts per liter. Additionally, the Grimm OPC has a lower flow rate of 1.2 lpm compared with the TSI OPC which has a flow rate of 2.8 lpm allowing for an even greater particle concentration to be accurately sampled. (GRIMM Aerosol Technik GmbH & Co., 2009)

The first objective of this research study was the evaluation of the effectiveness of several controls. The only statistically significant reduction in any of the metrics used in this study was seen when wetted water or water were utilized. This effectiveness was seen during the analysis of the idealize particle size distributions for burnt ACM tickets. The second objective of this research study was the generation of improved sampling procedures for ACM processes. The particle size distribution data generated by combining the OPC and CPC data and utilizing data correction strategy 3 was the best measure seen. While this procedure was based on a number of assumptions it was the best metric seen for evaluating exposures to composite fibers. Strategy 3's data correction procedure is not needed if the particle concentration does not exceed the linear region for the OPC used.

Future Studies

A depiction of the overall sampling efforts regarding composite fiber processes can be seen in Table 13.

Table 13 Areas of sampling strategy for composite fiber this study satisfies

		Level of process evaluation		
		Bench top simulation	Full process simulation	Process in the field
Process evaluated	Aircraft Disassembly	X		
	ACM panel handling			
	Walking around			
	Maintenance activities	X		

This study looked at aircraft disassembly after a crash. Other composite fiber processes that need to be evaluated within the Air Force are: handling ACM panels after a crash, inspection of a crash scene containing ACM, and maintenance activities on ACM panels and components. For these different processes there are three levels of process evaluation: bench top simulation of the process, full process simulation, and full process in the field. This study was a bench top simulation. A full process simulation would be a recreation of the process in a controlled environment. The final stage of sampling would be sampling of the process as it occurs in the field. Beyond the different processes and different levels of evaluation, different airframes will also need to be sampled. This is due to the fact that several aircraft contain ACM panels and these composites will have different stack ups depending on the specification of the aircraft. Additionally, both




epoxy and BMI composites would need to be sampled to determine if there are any differences between the two binding resins.

The purpose of this investigation was to evaluate aircraft disassembly during crash recovery operations. The results obtained also shed some light on the composite repair processes as intact tickets were cut during this study. These results would indicate that pretreatment controls would also not be effective for controlling the aerosolization of carbon fibers during maintenance processes.

These different areas of the potential sampling are not of equal importance when it comes to need for investigation. A judgment on the importance of these areas can be seen in Table 14 where cells in red are the highest priority, yellow cells are of moderate priority, and green cells are of lesser priority. This assessment was based on a subjective expectation of the degree of exposure and the frequency of the operation.

Table 14 Importance of different areas of potential sampling prior to this study

		Level of process evaluation		
		Bench top simulation	Full process simulation	Process in the field
Process evaluated	Aircraft Disassembly	High Priority (Red)	Medium Priority (Yellow)	Medium Priority (Yellow)
	ACM panel handling	Low Priority (Green)	Medium Priority (Yellow)	Low Priority (Green)
	Walking around	Low Priority (Green)	Medium Priority (Yellow)	Low Priority (Green)
	Maintenance activities	Medium Priority (Yellow)	Medium Priority (Yellow)	High Priority (Red)




Legend: Low Priority: 
 Medium Priority: 
 High Priority: 

This study looked at a bench top simulation of crash recovery aircraft disassembly. This was accomplished first due to the fact that the active cutting of potentially burnt aircraft was seen as the most hazardous of the operations. A bench top simulation was used in this study due the fact that a full process simulation was not feasible with the information on hand at the time. Additionally, the frequency of aircraft crashes could not be predicted and holding up evaluation of these processes until such an incident occurred was not a desirable option.

With the lessons learned during this bench top simulation a full process simulation would now be feasible and worthwhile. A reprioritized ranking of the different areas of sampling on ACM materials can be seen in Table 15.

Table 15 Priority of future sampling of ACM within the Air Force

		Level of process evaluation		
		Bench top simulation	Full process simulation	Process in the field
Process evaluated	Aircraft Disassembly	Green	Yellow	Yellow
	ACM panel handling	Green	Yellow	Green
	Walking around	Green	Yellow	Green
	Maintenance activities	Green	Yellow	Red

Legend: Low Priority: 
 Medium Priority: 
 High Priority: 

The highest priority is the sampling of the repair of ACM panels within the Air Force as these processes are currently being accomplished. Full process simulation of aircraft disassembly is of moderate priority but the next logical step in composite process

evaluation. Concurrently, preparation for the sampling of an aircraft crash should be implemented.

ACM panels are present on a number of airframes within the inventory and require replacement when they are damaged. TO 1-1-690 recommends the use of a kett (rotary) saw with a diamond blade or a router with a diamond bit for the removal of ACM panels with large or moderate damage respectively. (US Air Force, 2007) Due to the frequency of these processes it should be relatively simple to organize a sampling campaign to determine the potential exposures during this work. The TO recommends the use of vacuum equipment if it is available. This type of LEV has been shown to be useful for concrete work but these studies had vacuum hoses attached directly to a hood that was in place around the blade. Simple vacuum hoses next to the cutting surface may not be as effective. The effectiveness of the vacuum systems that are used by maintenance personnel should be evaluated and a standardized setup recommended for Air Force wide use. Cooling water controls may not be feasible for aircraft maintenance work due to the electronics on the aircraft and the lack of a capture system for the water after it is sprayed.

A full process simulation would allow for a controlled experiment to take place where external factors could be controlled when possible. Additionally, the larger facility would allow for less simulation of the aircraft disassembly process and provided exposure data that is more in line with real-world exposures. A facility such as the burn facility at Tyndall AFB used during the HAMMER studies would be an ideal location. In such a facility, full size ACM components could be burned and experimented on. Use of full size ACM panels would allow for the cutting of the ACM panels to be performed

with concrete saws that are used during real world operations. Similar to this study, samples should be performed during cutting of burnt and intact tickets. Also, samples should be taken for the baseline condition of no control as well as the LEV and active water spraying controls.

In addition to these first tier sampling priorities, sampling of an aircraft crash should be performed if possible. To achieve this, it is recommended that the USAFSAM be added to the notification checklist for an aircraft crash. This would allow for the rapid deployment of a one or two person team to the site of the aircraft crash to conduct a sampling campaign during the post crash investigation and recovery. A preassembled sampling kit with the needed media and equipment should be maintained so that it can be rapidly sent to the incident site. Such a kit would need to have a multitude of sampling filters, pumps, and DRIs as well as sampling accessories. This kit is needed so that any type of crash or other issue can be taken into account and compensated for so that representative sampling can be performed. Such an inventory would at a minimum consist of: sample pumps, preweighed PVC filters, MCE filters, aluminum cyclones, tygon tubing, tubing connectors, sample holders, OPC, CPC, CPC dilution setup, surface area meter, and appropriate SEM/TEM media.

With the support of the local BE flight the sample team should sample a number of different personnel as well as perform a number of area samples. Personnel with a variety of activities should be sampled during entry to the incident site. Crash investigators who are walking through the crash site taking pictures and making notes of the crash site should be sampled to provide data on low activity entrants to the crash site. Maintenance personnel that are moving and packaging aircraft components should be

sampled to provide data on component movement not including disassembly. Additionally, crash recovery personnel that are actively disassembling the airframe should be sampled. These three types of entries should be sampled at a minimum so that actual exposure data can be gathered. Area samples should also be performed simultaneously at multiple distances from the crash site both up and down wind during the major stages of the management of the aircraft crash. This would allow for a more informed hazard distance to be determined for aircraft crashes.

Recommendations for BE Flights

Due to the findings of this study wetted water and water should be used as a control for airborne composite fiber during crash recovery operations. It may not be practical to spray the crash with wetted water at austere crash sites, but water is generally available. Water alone does also provide a significant benefit in the shift of the particle size distribution. This use of a wetted water or water control does not eliminate the need for respiratory protection. It does increase the effectiveness of the respirator during the cutting of burnt ACM panels. Wax spray should also continue to be used as a fixant to prevent resuspension of carbon fiber particles during site walkthrough and ACM component handling after a crash, although this study did not investigate the effectiveness of a wax spray for this application.

With the information this study provides, several recommendations for BE flights that support ACM aircraft can be made. BE flights should have preweighed PVC media on hand so that gravimetric samples can be performed. While their usefulness and absolute accuracy may be limited they would provide an easy, low cost means of

exposure measurement. Additionally, once the USAFSAM contract for TEM sampling is complete BE flights should have the appropriate media on hand for TEM sampling. It is currently not feasible for every BE flight to procure the DRIs used during this study. However, every BE flight has a number of TSI portacounts (TSI; Shoreview, MN) for respirator fit testing. These portacounts are CPCs identical in operation to the CPCs used during this study without the data logging capability and the interface of the PTrak. These instruments could be used to measure submicron particles in the air around a crash site when the count setting is selected. The portacount would also be useful for the sampling of the crash site so that better control decisions can be made.

Conclusions

ACM containing carbon fibers are increasing in usage within military aviation due to its strength and low weight. Carbon fibers and nanoparticles pose a number of hazards to human health. While the best exposure metric is yet to be determined, evaluation of a number of these metrics should still be accomplished. The increased usage of ACM panels has grown beyond just military applications as civilian airliners are taking advantage of their desirable properties. Due to this, a careful evaluation of the exposure is prudent. With these potential exposure metrics, controls can be evaluated. While the precise “safe” level is still unknown, reducing the level of exposure when possible would be prudent. This study looked at the simulated disassembly of aircraft after a crash to determine if pretreatment controls would be effective at reducing exposure to the aerosol generated during the cutting of burnt and intact ACM panels.

This study showed that a statistically significant shift in particle size distribution was produced when using the wetted water and water controls on burnt ACM tickets. These controls were able to shift the particle size distribution toward larger diameters that are more efficiently filtered by respirators and will settle more quickly. Additionally, the wax, water, and wetted water all showed some benefit for other metrics during the cutting of burnt ACM samples. With this in mind, wetted water and water spray of burnt ACM panels should be used to increase the effectiveness of respiratory protection used by workers actively cutting ACM panels. Additionally, usage of wax as a fixant during the inspection and handling of ACM panels should continue.

This study also provided experience in the sampling of carbon fiber ACM panels. Gravimetric and SEM sampling should not be attempted on the same filter. Gravimetric samples should use PVC filters whereas SEM/TEM samples should use the media recommended by the analyzing laboratory. If possible, TEM samples should be performed and analyzed by a dedicated laboratory due to need for good sample transfer and the high level of magnification provided by TEM analysis. The most useful DRI data was provided by a combining the OPC and CPC outputs to develop a more complete picture of the particle size distributions generated during composite processes. Also, particulate sampling should be performed with instruments with the highest available linearity limit to provide quality data at the highest possible particulate concentration.

The next step in the evaluation of ACM processes in the Air Force is the full process simulation of post-crash aircraft disassembly and the evaluation of routine maintenance of ACM panels. Aircraft disassembly is likely the most hazardous exposure to carbon fiber where as routine maintenance is likely the most common exposure to

carbon fiber within the Air Force. Due to this, these two processes are the highest priority for evaluation and control. If possible, a full sampling campaign should be performed on an aircraft crash in the field. Secondly, an evaluation of the handling and packaging of ACM panel fragments after a crash as well as resuspension of particle during an inspection of the crash site should be evaluated at a later date.

Appendix A

Table 16 CPC, Surface Area, Respirable Mass Concentration, Total Mass Concentration, and Respirable Fraction data used for statistics

Ticket Status	Control	Trial number	CPC (count/cc)	SAM ($\mu\text{m}^2/\text{cc}$)	Resp (mg/m^3)	Total (mg/m^3)	Resp/ Total
Burnt	AFFF	3	229504	105.34	10.73	342.72	0.0313
Burnt	AFFF	2	68992	80.28	18.90	174.70	0.1082
Burnt	AFFF	1	157134	85.64	10.60	162.32	0.0653
Burnt	Nothing	1	203207	99.74	12.50	347.74	0.0360
Burnt	Nothing	2	120053	51.95	16.95	308.40	0.0550
Burnt	Nothing	3	113232	76.22	9.79	314.29	0.0311
Burnt	Water	3	32651	42.18	11.76	134.66	0.0873
Burnt	Water	2	1959	24.52	9.20	203.96	0.0451
Burnt	Water	1	86654	75.54	8.01	254.43	0.0315
Burnt	Wax	2	207101	1323.17	17.52	250.27	0.0700
Burnt	Wax	1	46345	44.26	6.79	95.41	0.0712
Burnt	Wax	3	146886	67.92	7.48	155.05	0.0482
Burnt	Wetted water	1	57805	50.43	12.52	192.40	0.0651
Burnt	Wetted water	3	1020	17.21	15.17	184.65	0.0822
Burnt	Wetted water	2	2798	22.86	10.47	346.06	0.0302
Intact	AFFF	2	74734	58.21	12.90	369.80	0.0349
Intact	AFFF	1	139238	79.54	12.64	292.67	0.0432
Intact	AFFF	3	448808	83.55	11.96	554.43	0.0216
Intact	Nothing	1	151200	60.21	7.28	156.70	0.0465
Intact	Nothing	2	316093	126.44	12.66	192.81	0.0657
Intact	Nothing	3	158154	54.54	7.30	481.17	0.0152
Intact	Water	2	169772	87.06	9.88	337.96	0.0292
Intact	Water	1	223328	99.33	13.08	284.02	0.0461
Intact	Water	3	258119	141.41	12.89	323.79	0.0398
Intact	Wax	2	214030	148.67	9.35	252.49	0.0370
Intact	Wax	3	305542	175	9.24	313.31	0.0295
Intact	Wax	1	296879	152.57	10.87	223.87	0.0485
Intact	Wetted water	3	264924	136.2	10.49	177.23	0.0592
Intact	Wetted water	2	171277	132.06	17.76	299.50	0.0593
Intact	Wetted water	1	255565	159.76	13.00	218.88	0.0594

Table 17 OPC CMD, OPC MMD, OPC+CPC CMD (Strategy 1), and OPC+CPC MMD (Strategy 1) data used for statistics

Ticket status	Control	Trial Number	CMD	MMD	OPC+CPC CMD (Strat 1)	OPC+CPC MMD (Strat 1)
Burnt	AFFF	3	1.44	20.64	0.1627	0.1848
Burnt	AFFF	2	1.84	7.68	0.1699	0.2703
Burnt	AFFF	1	1.95	10.54	0.1650	0.2115
Burnt	Nothing	1	1.48	9.48	0.1632	0.1888
Burnt	Nothing	2	1.63	31.36	0.1632	0.1920
Burnt	Nothing	3	1.41	22.04	0.1640	0.1981
Burnt	Water	3	1.32	8.46	0.1744	0.3175
Burnt	Water	2	1.18	9.13	0.4231	22.8583
Burnt	Water	1	1.43	22.40	0.1650	0.2092
Burnt	Wax	2	1.68	14.15	0.1633	0.1919
Burnt	Wax	1	1.23	7.49	0.1687	0.2428
Burnt	Wax	3	1.38	9.48	0.1633	0.1891
Burnt	Wetted water	1	1.67	5.47	0.1704	0.2706
Burnt	Wetted water	3	1.48	9.91	0.8812	53.9810
Burnt	Wetted water	2	1.41	7.73	0.3595	18.6258
Intact	AFFF	2	0.86	11.89	0.1609	0.1667
Intact	AFFF	1	1.43	20.95	0.1636	0.1941
Intact	AFFF	3	1.39	24.66	0.1609	0.1685
Intact	Nothing	1	1.14	14.75	0.1625	0.1815
Intact	Nothing	2	1.49	23.46	0.1616	0.1746
Intact	Nothing	3	1.73	35.62	0.1629	0.1894
Intact	Water	2	1.30	21.69	0.1620	0.1778
Intact	Water	1	1.44	26.10	0.1619	0.1781
Intact	Water	3	1.72	29.45	0.1623	0.1826
Intact	Wax	2	1.60	20.30	0.1625	0.1838
Intact	Wax	3	1.61	22.88	0.1619	0.1782
Intact	Wax	1	1.50	22.78	0.1617	0.1758
Intact	Wetted water	3	1.50	22.61	0.1620	0.1790
Intact	Wetted water	2	2.08	18.21	0.1632	0.1925
Intact	Wetted water	1	1.27	19.76	0.1618	0.1758

Table 18 OPC+CPC CMD (Strategy 2), OPC+CPC MMD (Strategy 2), OPC+CPC CMD (Strategy 3), OPC+CPC MMD (Strategy 3) data used for statistics

Ticket status	Control	Trial number	OPC+CPC CMD (Strat 2)	OPC+CPC MMD (Strat 2)	OPC+CPC CMD (Strat 3)	OPC+CPC MMD (Strat 3)
Burnt	AFFF	3	0.1668	0.2296	0.1739	0.3586
Burnt	AFFF	2	0.1816	0.4717	0.1993	1.1500
Burnt	AFFF	1	0.1722	0.3082	0.1840	0.6178
Burnt	Nothing	1	0.1680	0.2401	0.1738	0.3368
Burnt	Nothing	2	0.1675	0.2427	0.1771	0.4488
Burnt	Nothing	3	0.1692	0.2591	0.1792	0.4786
Burnt	Water	3	0.1886	0.5690	0.2075	1.3040
Burnt	Water	2	0.5170	31.4068	0.7004	89.9957
Burnt	Water	1	0.1712	0.2862	0.1835	0.5947
Burnt	Wax	2	0.1683	0.2504	0.1763	0.4045
Burnt	Wax	1	0.1781	0.3639	0.1890	0.6123
Burnt	Wax	3	0.1678	0.2368	0.1735	0.3304
Burnt	Wetted water	1	0.1822	0.4606	0.1958	0.8867
Burnt	Wetted water	3	0.9996	41.4966	1.3409	76.5745
Burnt	Wetted water	2	0.4529	35.1909	0.6155	108.378
Intact	AFFF	2	0.1619	0.1750	0.1636	0.1938
Intact	AFFF	1	0.1685	0.2508	0.1776	0.4369
Intact	AFFF	3	0.1627	0.1851	0.1657	0.2274
Intact	Nothing	1	0.1660	0.2155	0.1660	0.2155
Intact	Nothing	2	0.1642	0.2017	0.1690	0.2748
Intact	Nothing	3	0.1671	0.2391	0.1768	0.4527
Intact	Water	2	0.1648	0.2063	0.1699	0.2859
Intact	Water	1	0.1650	0.2095	0.1707	0.3060
Intact	Water	3	0.1660	0.2243	0.1736	0.3714
Intact	Wax	2	0.1663	0.2260	0.1732	0.3491
Intact	Wax	3	0.1651	0.2123	0.1709	0.3082
Intact	Wax	1	0.1645	0.2047	0.1695	0.2840
Intact	Wetted water	3	0.1653	0.2136	0.1712	0.3113
Intact	Wetted water	2	0.1678	0.2497	0.1773	0.4597
Intact	Wetted water	1	0.1646	0.2036	0.1694	0.2755

Appendix B

Detailed Procedures

Cut Procedure

1. Pre calibrate pumps
2. Zero OPC
3. Plumb bag
4. Pre weight ticket
5. Apply control to ticket
6. Insert ticket into holder
7. Seal bag
8. Start samples on each instrument
 - a. Total
 - b. Resp
 - c. SAM
 - d. OPC
 - e. CPC
 - f. Dremel
 - i. Used cut off disk at the end of a dremel extension so that dremel not in bag
 - ii. 10000 rpm setting used tried 5000 rpm but blade bogs down, was not practical
9. 1 cut ~ 7 mm deep
 - a. Allow DRIs to complete sample (1 min from start)
10. 3 more cuts ~ 7 mm deep
 - a. Turn off dremel
11. Turn off total pump ~2 min
 - a. Early attempts showed that longer sampling times would overload filter so that collected particles would be disturbed during cassette disassembly
12. Turn off resp pump ~20 min
 - a. Early attempts showed that 20 min of sample was required for enough mass to be collected on filter
13. Remove cassettes from bag
14. Reseal bag
15. Disassemble cassettes and Weigh filters 4x each
 - a. Resp
 - i. Dirty

- ii. Clean
- b. Total
 - i. Dirty
 - ii. Clean
- 16. Reassemble cassettes with caps for later analysis
- 17. Remove ticket from bag
- 18. Post weight ticket
- 19. Disassemble Sample setup to prepare for next sample run
- 20. Post calibrate pumps

SEM Sample prep

Respirable mass filters were chosen to be looked at with the SEM. This is due to the fact that respirable mass will be deposited in the lungs and will not contain the larger aerosol particles that are present in the total mass samples. The samples for the SEM had to be prepared. The sample prep had three steps: copper preparation, carbon foil preparation, and sample affixation.

First, the copper plate used needed to be buffed and cleaned. To accomplish this, a dremel tool buffing wheel was used to buff both sides of the copper plate until it was smooth and brilliant. Methanol was used to clean both sides of the copper plate so that no grease or other contaminants were present.

Once the copper had been prepared and cleaned, the carbon foil had to be affixed to the copper. To accomplish this, a razor blade was used to cut the carbon foil from the roll. Forceps were then used to pick up the tape and set it down on the copper that had previously been prepared. The razor blade was then used to press down the carbon foil to make sure it was properly affixed to the copper plate.

With the carbon foil affixed to the copper plate the sample could then be applied. A razor blade was used to pick up a small clump of the mass collected on the respirable

filter. This sample was then set onto the carbon foil. Once on the carbon foil the razor blade was used to spread the sample around so a thin layer of the sample was spread on the carbon foil. To make sure the sample was securely affixed to the carbon foil the copper plate was stood on end and tapped. This was done so no loose carbon fibers were present as they would damage the SEM. A swab with methanol was then used to clean the copper plate surface that surrounded the carbon foil. A microscope was then used to verify the copper plate was clean and the sample had been affixed to the carbon foil. The razor blade and forceps were then cleaned with methanol and the process was repeated for each of the samples.

Appendix C

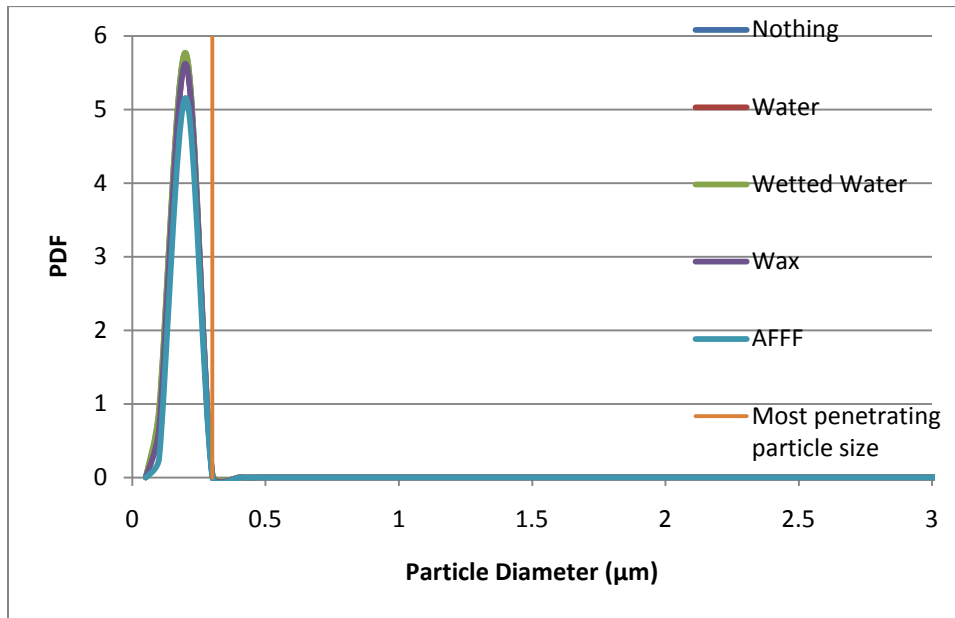


Figure 26 Plot of idealized particle size distributions for intact tickets based on CMD and CMD GSD (strategy 1) for different control options

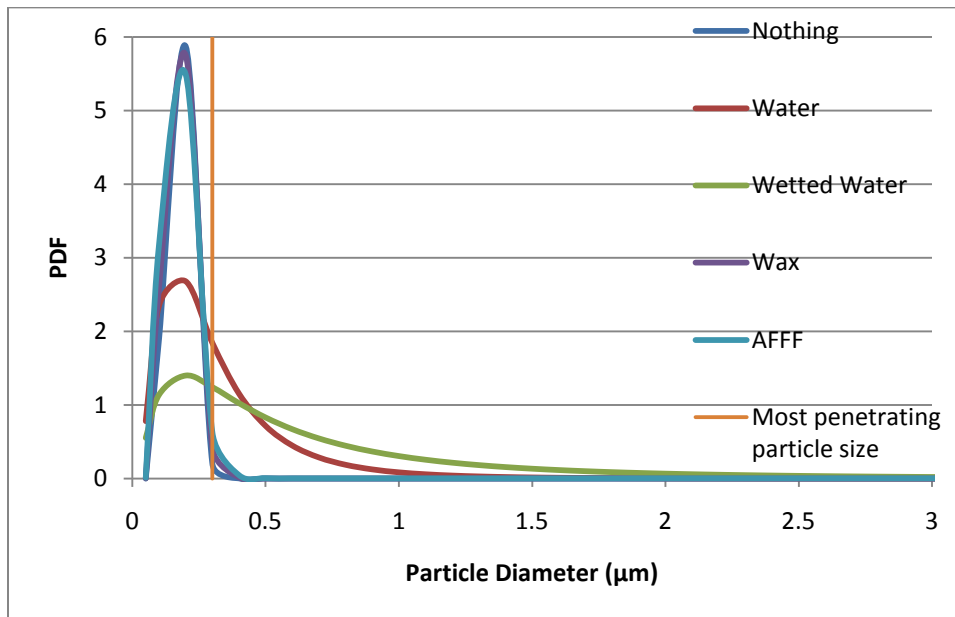


Figure 27 Plot of idealized particle size distributions for burnt tickets based on CMD and CMD GSD (strategy 1) for different control options

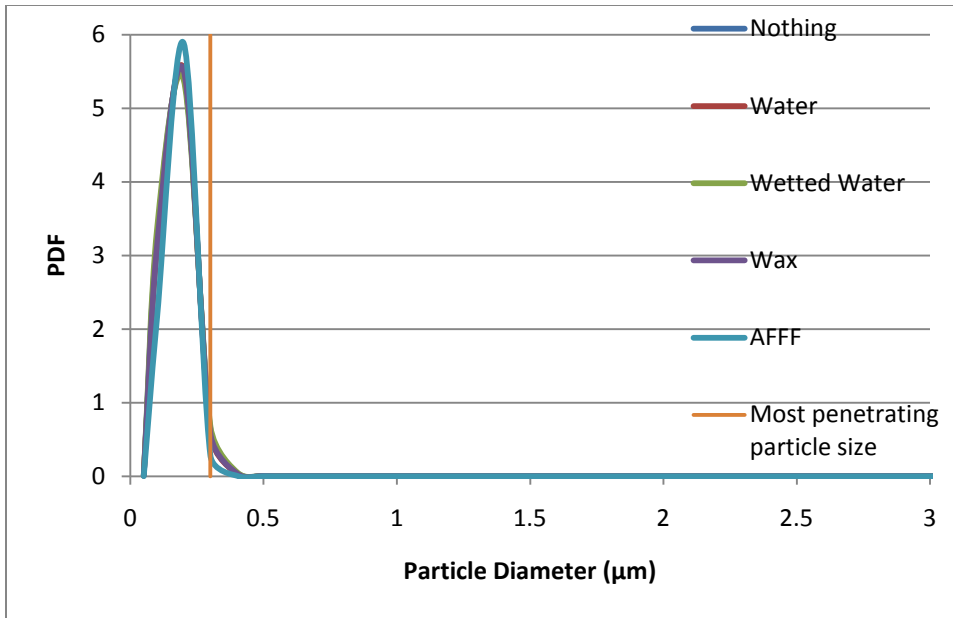


Figure 28 Plot of idealized particle size distributions for intact tickets based on CMD and CMD GSD (strategy 2) for different control options

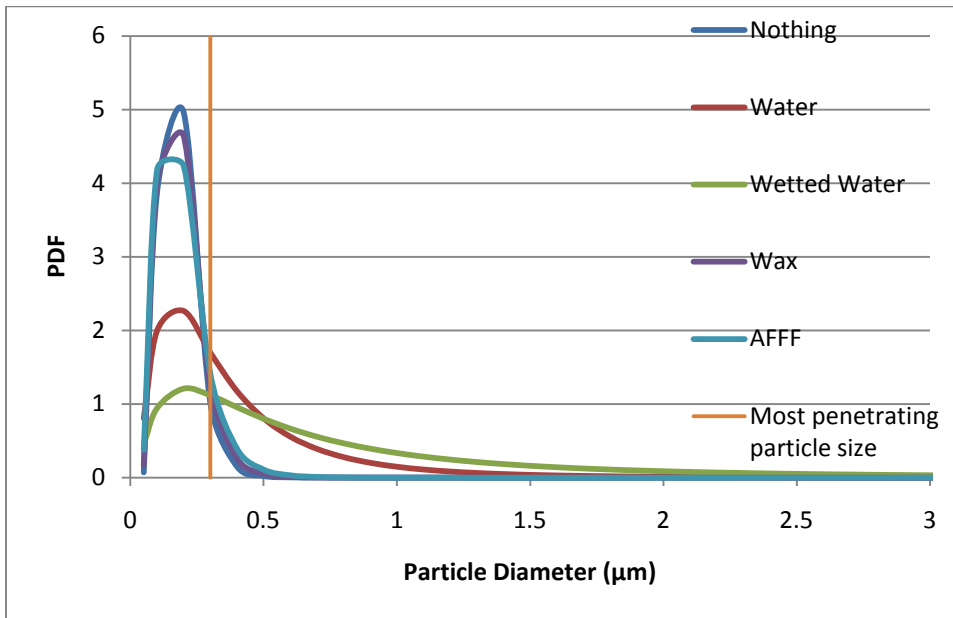


Figure 29 Plot of idealized particle size distributions for burnt tickets based on CMD and CMD GSD (strategy 2) for different control options

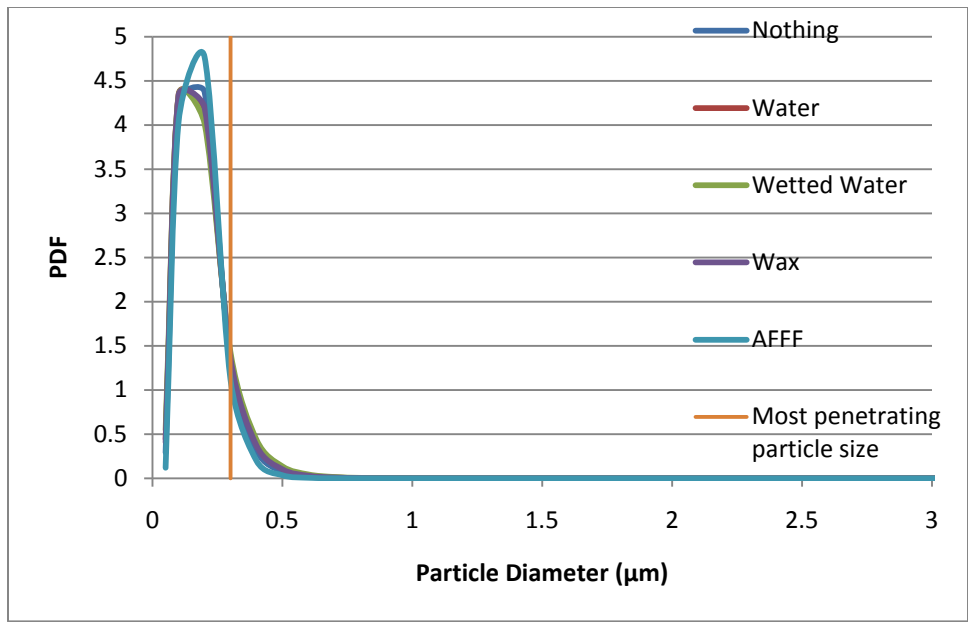


Figure 30 Plot of idealized particle size distributions for intact tickets based on CMD and CMD GSD (strategy 3) for different control options

Bibliography

- ACGIH. (2009). *TLVs and BEIs Based on the Documentation of the*. Cincinnati: ACGIH.
- AFIERA. (2001). *Assessment of Composite Hazards at Crash Sites: Industrial Hygiene Field Guidance For Bioenvironmental Engineers*. Brooks City-Base: US Air Force.
- AFIERA. (2001). *Characterization of Environmental and Health Exposures During a Composite Aircraft Fire and Simulated Aircraft Recovery Operations*. Brooks AFB: AFIERA.
- Air Force Advanced Composites Office. (n.d.). AC Inventory-Composites.
- Brown, N. (2009, December 1). Use of 3007 coincidence correction. (M. Ferreri, Interviewer)
- Cayce, W., O'Sullivan, D., & Lujan, W. (2008). The 36 MDG Response to the B-2 Mishap of February 2008. *2009 Team Aerospace Operational Solutions Course (12 Feb 2009)*. Brooks City-Base.
- Cohen, B. S., & Charles S. McCammon, J. (2001). *Air Sampling Instruments for evaluation of atmospheric contaminants, 9th edition*. Cincinnati: ACGIH.
- Costantino, J. (2010, January 5). Aircraft used in HAMMER study. (M. Ferreri, Interviewer)
- Courson, D. L., Flemming, C. D., Kuhlmann, K. J., Lane, J. W., Grabau, J. H., Cline, J. M., et al. (1996). *Smoke Production And Thermal Decomposition Products From Advanced Composite Materials*. Wright-Patterson AFB: US Air Force.
- Elder, A., Gelein, R., Silva, V., Feikert, T., Opanashuk, L., Carter, J., et al. (2006). Translocation of Inhaled Ultrafine Manganese Oxide Particles to the Central Nervous System. *Environmental Health Perspectives*, 114 (8), 1172-1178.
- Eninger, R. M., Honda, T., Reponen, T., McKay, R., & Grinshpun, S. A. (2008). What Does Respirator Certification Tell Us About Filtration of Ultrafine Particles? *Journal of Occupational and Environmental Hygiene*, 5 (5), 286-295.
- Ferreri, M., Slagley, J., & Felker, D. (2009). *Characterization of Advanced Composite Material Particles Released During Simulated Crash Recovery Operations*. AIHce. Toronto.
- Frank, B. (2009, July 6). Interview on Advanced Composite Office Evaluation of Controls. (M. Ferreri, Interviewer)
- Gandhi, S., Lyon, R., & Speitel, L. (1999). Potential Health Hazards from Burning Aircraft Composites. *Journal of Fire Sciences*, 17, 20-41.
- GRIMM Aerosol Technik GmbH & Co. (2009). *Model 1.109*. Retrieved Jan 20, 2010, from Grimm Aerosol: http://www.grimm-aerosol.com/downloads/IAQ/GrimmAerosolTechnik_IAQ_1109.pdf
- Heitbrink, W. A., Evans, D. E., Ku, B. K., Maynard, A. D., Slavin, T. J., & Peters, T. M. (2009). Relationships Among Particle Number, Surface Area, and Respirable Mass Concentration in Automotive Engine Manufacturing. *Journal of Occupational and Environmental Hygiene*, 6 (1), 19-31.
- Hinds, W. C. (1999). *Aerosol Technology: Properties, behavior, and measurement of airborne particles second edition*. New York: John Wiley and Sons, inc.

- ICRP. (1994). *International Commission on Radiological Protection Publication 66 Human Respiratory Tract Model for Radiological Protection*. Oxford: Elsevier Science Ltd.
- Kimmel, E. C., & Courson, D. L. (2002). Characterization of Particulate Matter in Carbon-Graphite/Epoxy Advanced Composite Material Smoke. *AIHA Journal* , 63, 413-423.
- Lam, C. W., James, J. T., McCluskey, R., & Hunter, R. L. (2004). Pulmonary Toxicity of Single-Wall Carbon Nanotubes in Mice 7 and 90 Days After Intratracheal Instillation. *Toxicological Sciences* , 77, 126-134.
- Lam, C. W., James, J. T., McCluskey, R., Arepalli, S., & Hunter, R. L. (2006). A Review of Carbon Nanotube Toxicity and Assessment of Potential Occupational and Environmental Health Risks. *Critical Reviews in Toxicology* , 36, 189-217.
- Maynard, A. D. (2006). Nanotechnology: The Next Big Thing, or Much Ado about Nothing. *Annals of Occupational Hygiene* , 51 (1), 1-12.
- Maynard, A. D., & Kuempel, E. D. (2005). Airborne nanostructured particles and occupational health. *Journal of Nanoparticle Research* , 7, 587-614.
- Mazzuckelli, L. F., Methner, M. M., Birch, M. E., Evans, D. E., Ku, B.-K., Crouch, K., et al. (2007). Case Study. *Journal of Occupational and Environmental Hygiene* , 4 (12), 37-41.
- Methner, M., Hodson, L., & Geraci, C. (2010). Nanoparticle Emission Assessment Technique (NEAT) for the Identification and Measurement of Potential Inhalation Exposures to Engineered Nanomaterials - Part A. *Journal of Occupational and Environmental Hygiene* , 7 (3), 127-132.
- Methner, M., Hodson, L., Dames, A., & Geraci, C. (2010). Nanoparticle Emission Assessment Technique (NEAT) for the Identification and Measurement of Potential Inhalation Exposures to Engineered Nanomaterials - Part B: Results from 12 Field Studies. *Journal of Occupational and Environmental Hygiene* , 7 (3), 163-176.
- Middaugh, B. (2009). *Assessment of Cut-Off Saw Control Methods for Respirable Particulate and Crystalline Silica During Highway Construction Applications*. West Lafayette: Purdue University.
- Mouritz, A. P. (2009). Review of Smoke Toxicity of Fiber-Polymer Composites Used in Aircraft. *Journal of Aircraft* , 46 (3), 737-745.
- Nij, E. T., Hilhorst, S., Spee, T., Spierings, J., Steffens, F., Lumens, M., et al. (2003). Dust Control Measures in the Construction Industry. *Annals of Occupational Hygiene* , 47 (3), 211-218.
- NIOSH. (2009). *Approaches to Safe Nanotechnology: managing health and safety concerns associated with engineered nanomaterials*. Retrieved from NIOSH: www.cdc.gov/noish/topics/nanotech/safenano/
- NIOSH. (2003). *Diesel Particulate Mater (as Elemental Carbon)*. Retrieved from NIOSH: <http://www.cdc.gov/niosh/docs/2003-154/pdfs/5040.pdf>
- NIOSH. (2005, September). *NIOSH Pocket Guide to Chemical Hazards - graphite (natural)*. Retrieved from CDC: <http://www.cdc.gov/niosh/npg/npgd0306.html>
- Nygaard, U. C., Hansen, J. S., Samuelsen, M., Alberg, T., Marioara, C. D., & Løvik, M. (2009). Single-Walled and Multi-walled Carbon Nanotubes Promote Allergic Immune Responses in Mice. *Toxicological Science* , 109 (1), 113-123.

- Nygaard, U. C., Samuelsen, M., Aase, A., & Løvik, M. (2004). The Capacity of Particles to Increase Allergic Sensitization Is Predicted by Particle Number and Surface Area, Not by Particle Mass. *Toxicological Sciences* , 82 (2), 515-524.
- Oberdörster, G., Maynard, A., Donaldson, K., Castranova, V., Fitzpatrick, J., Ausman, K., et al. (2005). Principles for characterizing the potential human health effects from exposure to nanomaterials: elements of a screening strategy. *Particle and Fibre Toxicology* , 2 (8).
- Oberdörster, G., Oberdörster, E., & Oberdörster, J. (2005). Nanotoxicology: An Emerging Discipline Evolving from Studies of Ultrafine Particles. *Environmental Health Perspectives* , 113 (7), 823-839.
- Oberdörster, G., Sharp, Z., Atudorei, V., Elder, A., Gelein, R., Kreyling, W., et al. (2004). Translocation of Inhaled Ultrafine Particles to the Brain. *Inhalation Toxicology* , 16 (6-7), 437-445.
- O'Shaughnessy, P. T., & Slagley, J. M. (2002). Photometer Response Determination Based on Aerosol Physical Characteristics. *AIHA Journal* , 63, 578-585.
- Poland, C. A., Duffin, R., Kinlock, I., Maynard, A., Wallace, W. A., Seaton, A., et al. (2008). Carbon nanotubes introduced into the abdominal cavity of mice show asbestos-like pathogenicity in a pilot study. *Nature nanotechnology* , 3, 423-428.
- Proctor, A., & Sherwood, P. (1982). X-ray Photoelectron Spectroscopic Studies of Carbon Fibre Surfaces. I. Carbon Fibre Spectra and the Effects of Heat Treatment. *Journal of Electron Spectroscopy and Related Phenomena* , 27, 39-56.
- Shvedova, A. A., Kisin, E., Mercer, R., Murray, A., Johnson, V., Potapovich, A., et al. (2005). Unusual inflammatory and fibrogenic pulmonary responses to single-walled carbon nanotubes in mice. *American Journal of Physiology - Lung Cellular and Molecular Physiology* , 289, 698-708.
- Storage, K. (2009, August 19). Composite ticket makeup. (M. Ferreri, Interviewer)
- Sussholtz, B. (1980). *Evaluation of Micron Size Fiber Release From Burning Graphite Composites*. Hampton: NASA.
- Tinkle, S. S., Antonini, J. M., Rich, B. A., Roberts, J. R., Salmen, R., DePree, K., et al. (2003). Skin as a Route of Exposure and Sensitization in Chronic Beryllium Disease. *Environmental Health Perspectives* , 111 (9), 1201-1208.
- Trakumas, S., & Hall, P. (2003). Performance Assessment of Personal Respirable Cyclone Samplers. *AIHce*. Dallas.
- TSI. (2006). *AeroTrak 8220 specification sheet*. Retrieved from TSI: http://www.tsi.com/uploadedFiles/Product_Information/Literature/Spec_Sheets/AER_OTRAK_Handheld-8220.pdf
- TSI. (2006). *AeroTrak 9000 product brochure*. Retrieved from TSI: http://www.tsi.com/uploadedFiles/Product_Information/Literature/Brochures/AeroTrak.pdf
- TSI. (2001). Coincidence Correction of Model 3007.
- TSI. (2007). *Ptrak 8525 specification sheet*. Retrieved from TSI: http://www.tsi.com/uploadedFiles/Product_Information/Literature/Spec_Sheets/PTrakSpec2980453.pdf
- US Air Force. (2008). *T.O. 00-105E-00, Aerospace Emergency Rescue and Mishap Response Information (Emergency Services)*.

- US Air Force. (2007). *T.O. 1-1-690 General Advanced Composite Repair Processes Manual*. US Air Force.
- Wilson, W. E., Stanek, J., Han, H.-S., Johnson, T., Sakurai, H., Pui, D. Y., et al. (2007). Use of the Electrical Aerosol Detector as an Indicator of the Surface Area of Fine Particles Deposited in the Lung. *Journal of Air & Waste Management Association* , 57, 211-220.
- Zhang, Z., Wang, X., Lin, L., Xing, S., Wu, Y., Li, Y., et al. (2001). The Effects of Carbon Fibre and Carbon Fibre Composite Dusts on Bronchoalveolar Lavage Components of Rats. *Journal of Occupational Health* , 43, 75-79.

REPORT DOCUMENTATION PAGE

Form Approved
OMB No. 074-0188

The public reporting burden for this collection of information is estimated to average 1 hour per response, including the time for reviewing instructions, searching existing data sources, gathering and maintaining the data needed, and completing and reviewing the collection of information. Send comments regarding this burden estimate or any other aspect of the collection of information, including suggestions for reducing this burden to Department of Defense, Washington Headquarters Services, Directorate for Information Operations and Reports (0704-0188), 1215 Jefferson Davis Highway, Suite 1204, Arlington, VA 22202-4302. Respondents should be aware that notwithstanding any other provision of law, no person shall be subject to a penalty for failing to comply with a collection of information if it does not display a currently valid OMB control number.

PLEASE DO NOT RETURN YOUR FORM TO THE ABOVE ADDRESS.

1. REPORT DATE (DD-MM-YYYY) 3/25/2010		2. REPORT TYPE Master's Thesis		3. DATES COVERED (From - To) Oct 2008 - Mar 2010	
4. TITLE AND SUBTITLE Particulate Characterization and Control Evaluation for Carbon Fiber Composite Aircraft Crash Recovery Operations			5a. CONTRACT NUMBER		
			5b. GRANT NUMBER		
			5c. PROGRAM ELEMENT NUMBER		
6. AUTHOR(S) Ferreri, Matthew, R., Capt, USAF			5d. PROJECT NUMBER N/A		
			5e. TASK NUMBER		
			5f. WORK UNIT NUMBER		
7. PERFORMING ORGANIZATION NAMES(S) AND ADDRESS(S) Air Force Institute of Technology Graduate School of Engineering and Management (AFIT/EN) 2950 Hobson Way WPAFB OH 45433-7765			8. PERFORMING ORGANIZATION REPORT NUMBER AFIT/GIH/ENV/10-M01		
9. SPONSORING/MONITORING AGENCY NAME(S) AND ADDRESS(ES) Air Force Advanced Composites Office Larry Coulter, Civ, Ch, AF Advanced Composite Office DSN 586-3319 5851 F Ave Bldg 849, Rm B-46 Hill AFB, UT 84056-5713			10. SPONSOR/MONITOR'S ACRONYM(S) AFRL/RXS-OLH		
			11. SPONSOR/MONITOR'S REPORT NUMBER(S)		
12. DISTRIBUTION/AVAILABILITY STATEMENT APPROVED FOR PUBLIC RELEASE; DISTRIBUTION UNLIMITED					
13. SUPPLEMENTARY NOTES This material is declared a work of the U.S. Government and is not subject to copyright protection in the United States					
14. ABSTRACT Within the United States Air Force (USAF) Advanced Composite Material (ACM) is gaining an increasing use in military aircraft. With the number of aircraft that have increasingly large amounts of ACM materials, the probability of an incident with one of these aircraft also increases. When such an incident occurs the aircraft needs to be disassembled, removed, and later inspected as part of the accident investigation process. This disassembly process is termed "Crash Recovery Operations." Carbon fibers have been shown to be hazardous to human health and a pilot study raised the suspicion that nanosized aerosol may be generated during the cutting of carbon fiber panels. Due to this, a bench top study was conducted to evaluate the effectiveness of several fiber controls. Additionally, an evaluation of a number of direct reading instruments and traditional gravimetric sampling techniques were evaluated to determine a sampling protocol for evaluation composite fibers. A statistically significant (F-value = < 0.0001) shift towards larger diameters in the idealized particle size distribution was shown for both wetted water and water controls when compared to a baseline of no control when cutting burnt ACM. Recommendations for future evaluation and control of composite fiber processes were made.					
15. SUBJECT TERMS Industrial Hygiene, Composite Fiber, Carbon Fiber, Particle Characterization					
16. SECURITY CLASSIFICATION OF:		17. LIMITATION OF ABSTRACT UU	18. NUMBER OF PAGES 107	19a. NAME OF RESPONSIBLE PERSON Jeremy M. Slagley, Maj, USAF (ENV)	
a. REPORT U	b. ABSTRACT U			c. THIS PAGE U	19b. TELEPHONE NUMBER (Include area code) (937) 255-3636, ext 4511; e-mail: Jeremy.Slagley@afit.edu

Standard Form 298 (Rev. 8-98)
Prescribed by ANSI Std. Z39-18

Form Approved
OMB No. 074-0188